Published by Avanti Publishers

Global Journal of Earth Science and Engineering

ISSN (online): 2409-5710

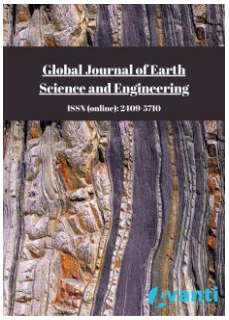

A Comprehensive Analysis of Water Budget Components and Water Yield in the Upper Awash Sub-Basin, Central Ethiopia Using the SWAT Model

Muauz A. Redda[1,*], Behailu B. Wolde[2], and Bedru H. Mohammed[3]

[1]*Ethiopian Institute of Water Resource, Addis Ababa University, Addis Ababa, Ethiopia*

[2]*School of Earth Sciences, Addis Ababa University, Addis Ababa, Ethiopia*

[3]*School of Earth Sciences and Engineering, Addis Ababa Science and Technology University, Addis Ababa, Ethiopia*

ARTICLE INFO

Article Type: Research Article

Academic Editor: Akinniyi Akinsunmade

Keywords:
SWAT model
Groundwater recharge
Water yield estimation
Upper awash sub-basin
Model calibration and validation
Hydrological modeling in Ethiopia

Timeline:
Received: May 27, 2025
Accepted: July 24, 2025
Published: August 25, 2025

Citation: Redda MA, Birhanu B, Mohammed BH. A comprehensive analysis of water budget components and water yield in the upper awash sub-basin, Central Ethiopia using the SWAT model. Glob J Earth Sci Eng. 2025; 12: 30-56.

DOI: https://doi.org/10.15377/2409-5710.2025.12.3

ABSTRACT

This study employed the Soil and Water Assessment Tool (SWAT) model to analyze the water budget components and water yield of the Upper Awash River sub-basin in Central Ethiopia. Utilizing data from 1986 to 2013, the model was calibrated from 1988 to 2008 following a three-year warm-up period and subsequently validated over five years at two gauging stations. Sensitivity analyses were conducted using t-stat and p-values, while model uncertainty was assessed using the p-factor and r-factor indices. The model's performance was evaluated using Nash-Sutcliffe efficiency (NSE), coefficient of determination (R^2), and Percent Bias (PBIAS). Calibration results yielded p-factors and r-factors of 0.801 and 0.9 for Hombele, and 0.808 and 0.98 for Melkakuntro. The calibration R^2, NSE, and PBIAS values were 0.82, 0.82, and-2.3, respectively, for Hombele, and 0.79, 0.78, and-13.1, respectively. Validation R^2, NSE, and PBIAS values were 0.71, 0.67, 11.2 for Hombele, and 0.7, 0.66, 1.9 for Melkakuntro. The average annual groundwater recharge rate ranged from 0 to 904.3 mm, averaging 181.1 mm/yr, which accounts for 19.1% of the mean annual rainfall. The simulated mean annual surface runoff and evapotranspiration were 93.4 mm and 682.5 mm, respectively, constituting 9.8% and 71.8% of the mean annual rainfall. The average annual water yield of the study area was 233.4 mm. These findings provide important insights into the hydrological dynamics of the Upper Awash River sub-basin, deepening our understanding of this water system. This information is essential for establishing sustainable water management practices and optimizing resource use for socioeconomic growth.

*Corresponding Author
Email: muauzamare79@gmail.com

1. Introduction

Sustainable management of water resources has become increasingly challenging owing to the uneven distribution of water and the rapidly growing demand driven by factors such as population growth, urbanization, industrialization, and agricultural expansion [1, 2]. In many regions, especially those prone to water scarcity, these pressures exacerbate the already strained water systems.

Ethiopia, located in the Horn of Africa, faces significant challenges in managing its water resources, owing to its diverse meteorological and geographical characteristics. The country's varied topography and rainfall patterns contribute to the uneven distribution of water resources [3]. In arid and semi-arid regions, the link between precipitation and aquifer recharge is often characterized by high spatial and temporal variability. Recharge occurs primarily during intense, short-duration rainfall events, with mechanisms including focused recharge through ephemeral streambeds, and diffuse infiltration. Factors such as vegetation cover, soil texture, and landform influence the recharge efficiency. Studies from regions including North Africa, the Middle East, and Central Australia have revealed that even minimal rainfall can contribute significantly to recharge under favorable conditions. This variability complicates efforts to ensure sustainable water management, especially in regions such as the Upper Awash River sub-basin in central Ethiopia, which is a vital watershed that provides water for domestic, agricultural, and industrial uses. However, the area is experiencing increasing water scarcity owing to rapid population growth, agricultural expansion, and climate change [4-6]. Urbanization and industrialization further intensify water demand, highlighting the urgent need for effective management strategies.

The total water yield, which represents the total volume of water exiting a given hydrological unit and contributing to the downstream flow, is a critical component for understanding the overall water balance within a watershed. It is an essential metric for assessing the availability of water resources for various uses such as agriculture, industry, and urban supply, particularly in regions experiencing water scarcity [7]. Studies have shown that an accurate estimation of water yield is vital for sustainable water resource management, as it helps identify the quantity of water that can be reliably extracted from a watershed without adversely affecting the ecosystem or downstream users [8].

Previous studies across global and Ethiopian river basins have examined water budget components, with a focus on availability, usage, and management under increasing anthropogenic and climatic pressures. For example, in Ethiopia [9, 10], rainfall variability and hydrological responses to land use and climate change have been explored using models, such as SWAT. Similarly, [11, 12], [13], and [14] conducted regional-scale assessments of flow dynamics and water yield, offering insights into basin-level resource allocation. On a broader scale, studies by [15-17] analyzed global water stress patterns, emphasizing the implications of climate variability on hydrological regimes. Hydrological modeling techniques, often integrated with remote sensing and geospatial analysis [18-20], have facilitated the quantification of key components, such as precipitation, evapotranspiration, runoff, and recharge. In the context of Eastern Africa, contributions by [21] and [22] provide evidence of groundwater-surface water interactions and modeled water scarcity scenarios. Collectively, these works underscore the necessity of incorporating spatiotemporal variability and climate-induced uncertainty into sustainable water resource planning in Ethiopia, which has traditionally been performed on a lumped scale and can result in inaccurate estimates of water volume in specific hydrological components. To address this limitation, it is essential to develop a methodology that accurately simulates the spatial distribution of the available and required water within a basin, considering the assumptions and constraints of global water budget models. Such methodologies are crucial for supporting decision-making processes that aim to ensure sustainable water resource management [23].

This study focuses on developing a spatially semi-distributed water budget model for the Upper Awash sub-basin using daily hydrometeorological data. The model is grounded in geographic information systems (GIS) and calculates groundwater recharge, surface runoff, evapotranspiration, and water yield based on variables such as land use, soil texture, topography, and hydrometeorological data. By providing a detailed understanding of the hydrological dynamics of this economically and socially significant region, this study aims to offer critical insights into sustainable water management practices. Despite existing research, a comprehensive understanding of the spatial distribution of water budget components in the upper wash sub-basin using long-term calibrated SWAT

modeling remains limited. This study aimed to fill this gap by applying the SWAT model to estimate groundwater recharge, surface runoff, evapotranspiration, and water yield using spatially explicit data and robust calibration techniques. The novelty of this study lies in its use of long-term data (1986-2013) for calibration and validation, which enhances the reliability and robustness of the findings. Additionally, the incorporation of advanced sensitivity analyses and model uncertainty assessments, complex volcanic terrain, and large areas that are not commonly included in similar studies, advanced hydrological modeling techniques provide a foundation for improved water management strategies in the region.

Hydrological models such as the Soil and Water Assessment Tool (SWAT) are crucial for evaluating and managing water resources by simulating various water-related processes and predicting the potential impacts of future climate and land-use changes [24].

These studies significantly contribute to the understanding of the regional and temporal variability of water resources and inform the development of management strategies and policies. They also highlight the need to account for the effects of climate change on the sustainability and availability of water resources in Ethiopia.

The objectives of this study were as follows:

(i) To estimate and evaluate the major water budget components (recharge, runoff, evapotranspiration, and yield) in the Upper Awash sub-basin using the SWAT model.

(ii) Assessing spatial and temporal variations in these components.

(iii) Calibration and validation of the model outputs using performance indices.

(iv) Perform sensitivity and uncertainty analyses to identify the key influencing parameters.

The remainder of this paper is structured as follows: Section 2 describes the study area and methodology; Section 3 presents the results and discussion, including model performance and water budget analysis; and Section 4 summarizes the main findings and provides recommendations.

2. Materials and Methods

2.1. Description of the Study Area

The Upper Awash River Sub-Basin, which covers an area of 11,697 km², is situated in Central Ethiopia Fig. (**1**) and is part of the larger Awash River Basin. It is bordered by mountainous terrain to the west and rift valley depressions to the east. The elevation in this region varies significantly, ranging from 1,579 m to 3,557 m above sea level. The area experiences a unimodal rainfall pattern, with an average annual precipitation of 1,078 mm and average annual temperature of 18.6°C.

The spatial distribution of mean annual precipitation, spanning the period from 1986 to 2013, within the Upper Awash River Sub-Basin was meticulously derived using discrete point data acquired from meteorological stations and subsequently interpolated through the application of the Inverse Distance Weighted (IDW) methodology. As depicted in Fig. (**2**), the basin demonstrates conspicuous spatial heterogeneity in its rainfall patterns. The annual precipitation values fluctuated considerably, ranging from approximately 775 mm to 1326 mm. The highest precipitation levels were observed within the southwestern and northern highland regions, which may be attributable to orographic influence. Conversely, the central, southern, and eastern zones manifest low precipitation levels, a phenomenon potentially governed by rain-shadow dynamics and topographic shielding. IDW interpolation effectively delineates these spatial gradients, thereby elucidating the profound impact of topography, elevation, and proximity to meteorological stations on the distribution of rainfall throughout the basin. This inherent heterogeneity in precipitation patterns has significant implications for hydrological modeling, the generation of surface runoff, , and the strategic allocation of water resources within the basin.

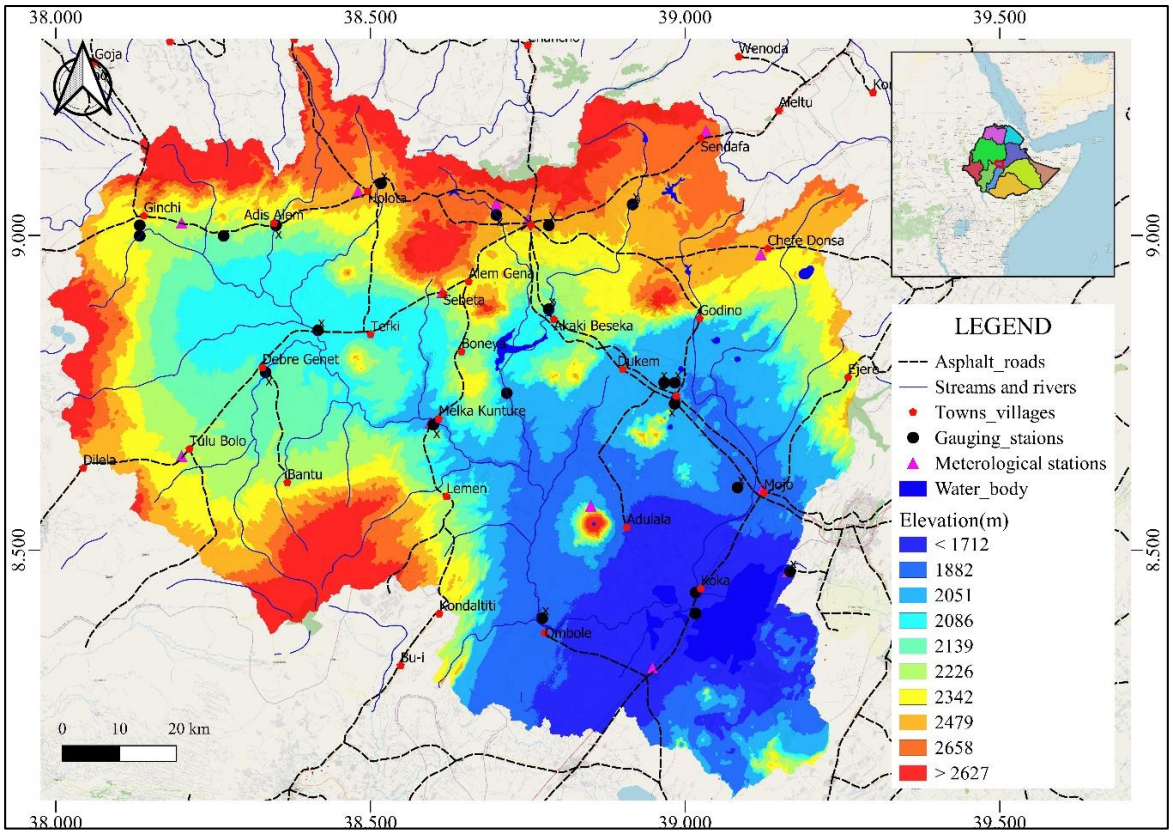

Figure 1: Location, elevation, gauging and meteorological stations map of the study area.

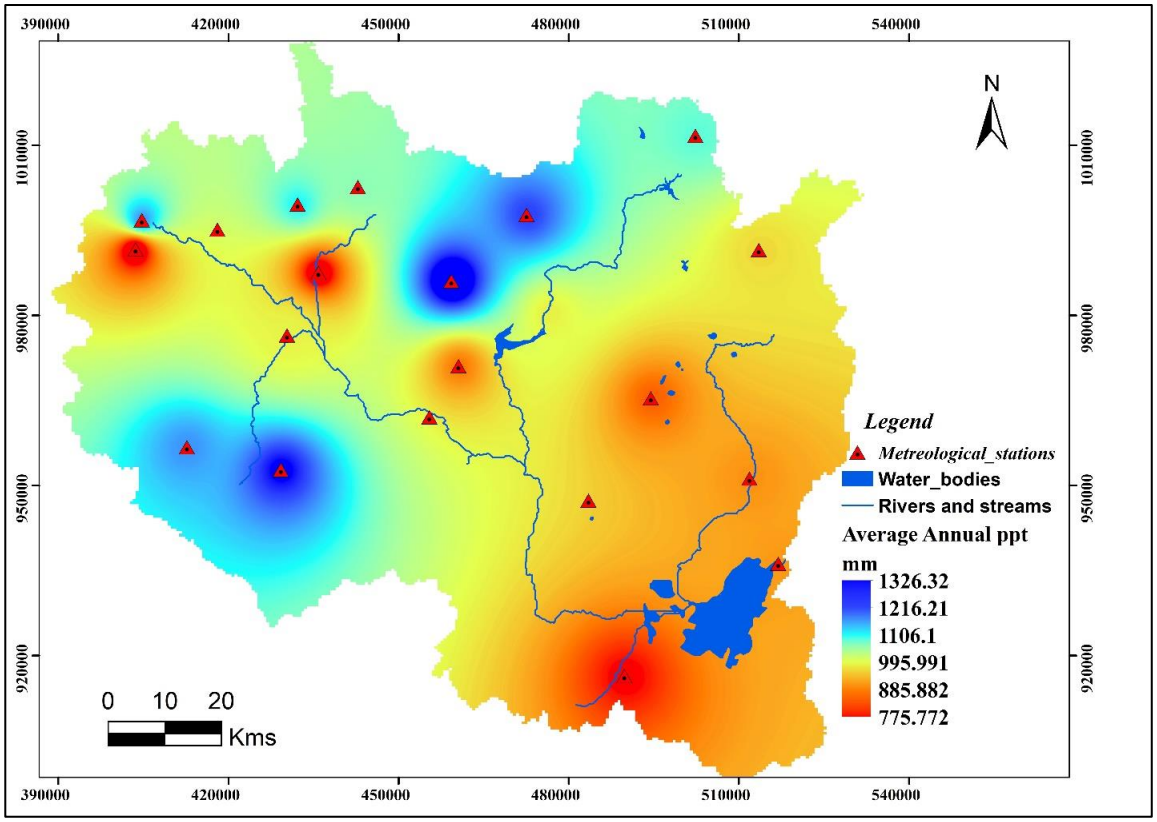

Figure 2: Describing the spatial distribution of average annual precipitation (1986-2013) across the Upper Awash River Sub-Basin, derived from station data and Inverse Distance Weighted (IDW) interpolation.

In terms of hydrology, the Awash River and its major tributaries, including the Akaki and Mojo Rivers, drain into the basin. Streamflow is monitored at key stations such as Hombole and Melkakuntro. The hydrological regime of this area is characterized by seasonal variability, with peak discharges occurring during the main rainy season, which lasts from June to September.

The lithostratigraphic units of the sub-basin are notably characterized by Tertiary-Quaternary volcanic rocks covering a substantial area. Additionally, minor intertrappean sediments, quaternary lacustrine sediments, and surface deposits were identified. Primary groundwater reservoirs were found within the fractured regions of volcanic rocks. The flowchart is shown in (Fig. **3**) provides a comprehensive overview of the methodological framework adopted for this study, illustrating the sequential steps and processes involved in analyzing the hydrological dynamics of the Upper Awash River sub-basin.

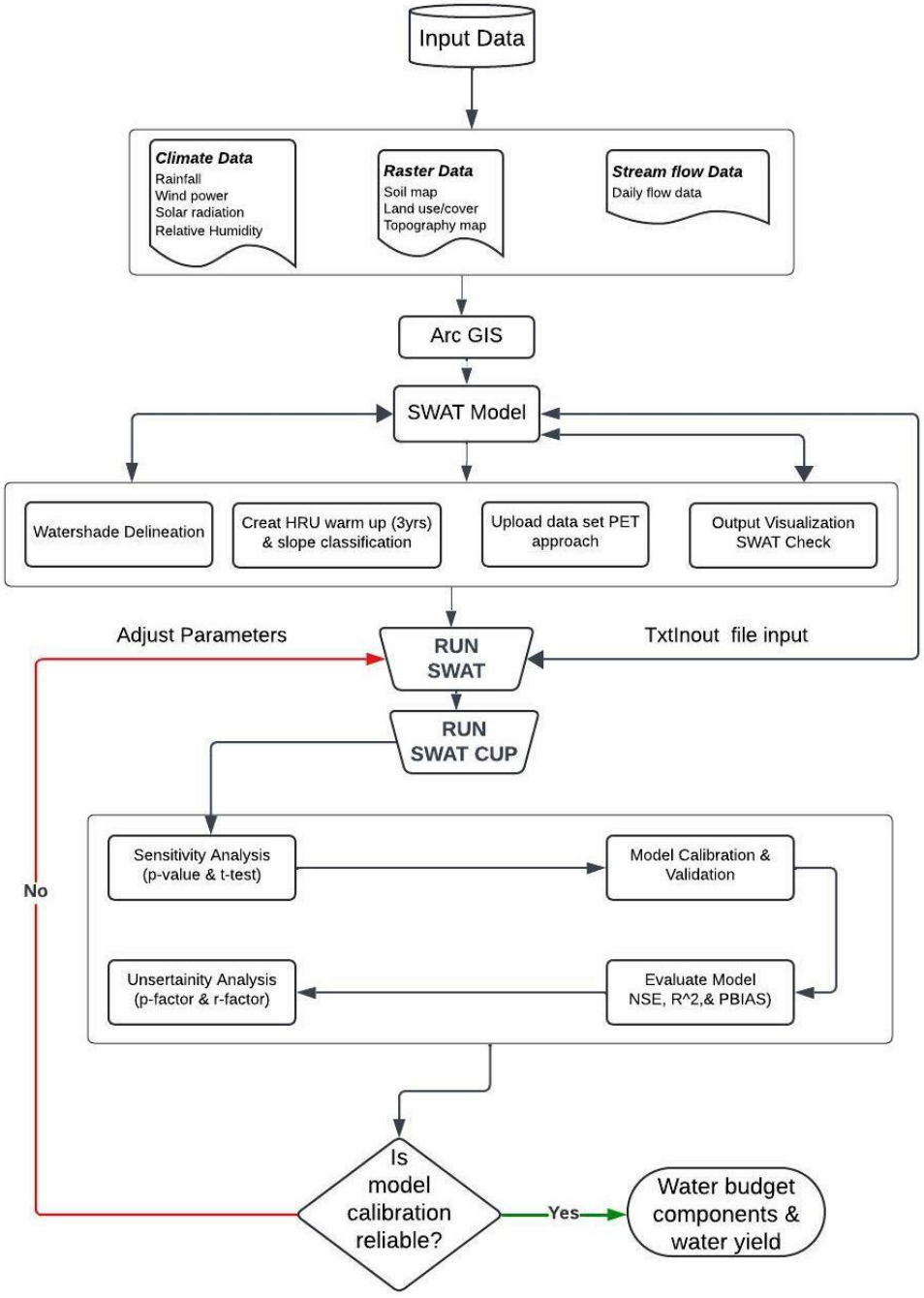

Figure 3: A flowchart to describe the methodology.

Geomorphology: The basin is located within the Ethiopian Highlands and the Central Rift Valley and is characterized by rugged hills, plateaus, and deeply incised valleys. The slopes varied significantly, with over 40% of the area classified in the 0-5% slope category (Fig. **4**). This terrain has a substantial impact on the surface runoff and infiltration dynamics.

Soils: The primary soil types in the basin included Eutric Vertisols (49.8%), Haplic Phaeozems, Cambisols, and Nitosols. These soils exhibit varying hydrological properties such as infiltration capacity and available water content, which play crucial roles in influencing runoff and groundwater recharge (Fig. **5**).

Land Use: Agricultural land constitutes 69.1% of the basin, followed by rangelands, forests, urban areas, and water bodies (Fig. **6**). The various land cover types affected hydrological responses and were utilized to define hydrological response units (HRUs) in the Soil and Water Assessment Tool (SWAT).

2.2. Model Description

The Soil and Water Assessment Tool (SWAT) is a semi-distributed, process-based model that simulates the impact of land use and climate variability on watershed hydrology [7]. It divides a watershed into sub-basins and Hydrologic Response Units (HRUs) based on land use, soil, and slope, allowing the spatially explicit simulation of hydrological processes.

In this study, SWAT was used to simulate the streamflow, surface runoff, evapotranspiration, groundwater recharge, and water yield. Surface runoff was estimated using the modified SCS Curve Number method, while evapotranspiration was calculated using the Penman–Monteith method, which requires inputs such as temperature, solar radiation, wind speed, and humidity [25]. Percolation, lateral flow, and base flow were simulated through soil-layer interactions and shallow aquifer contributions [26].

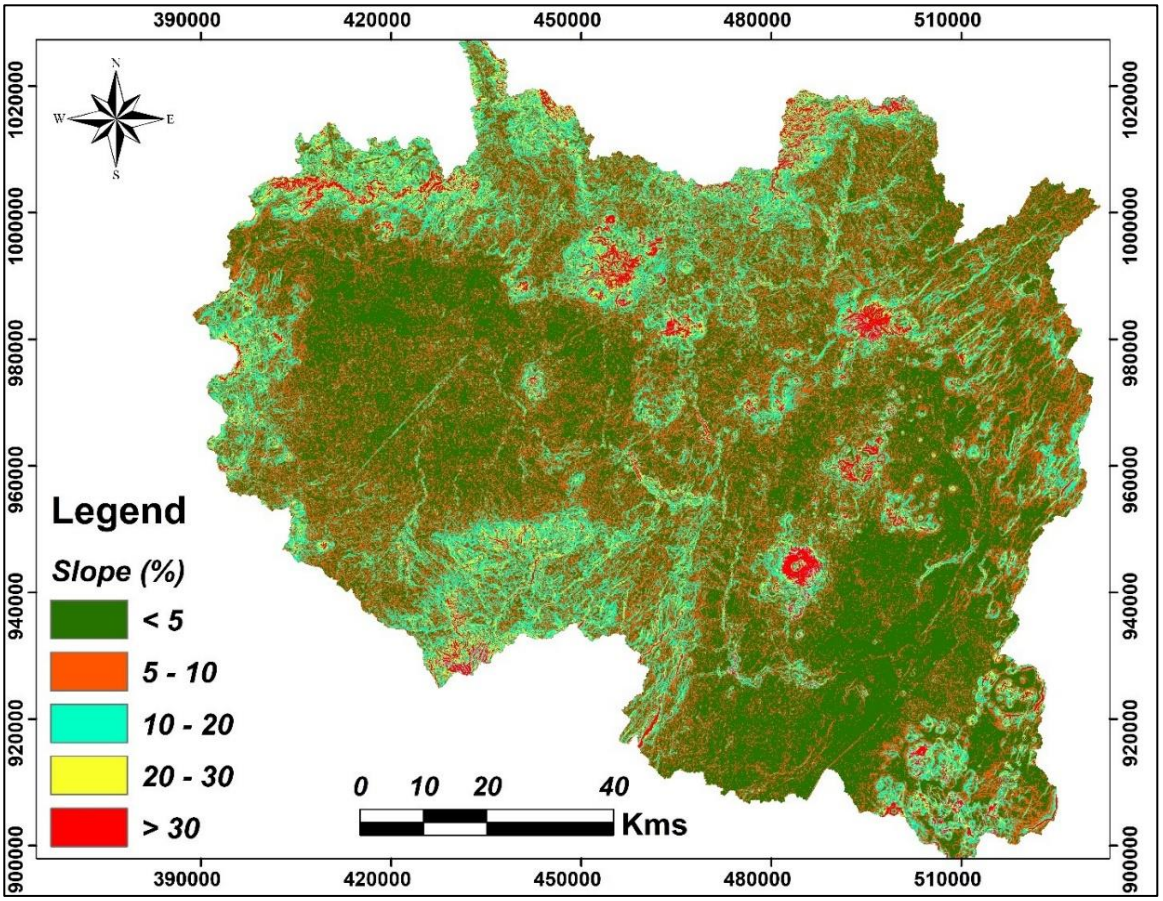

Figure 4: Slope classification.

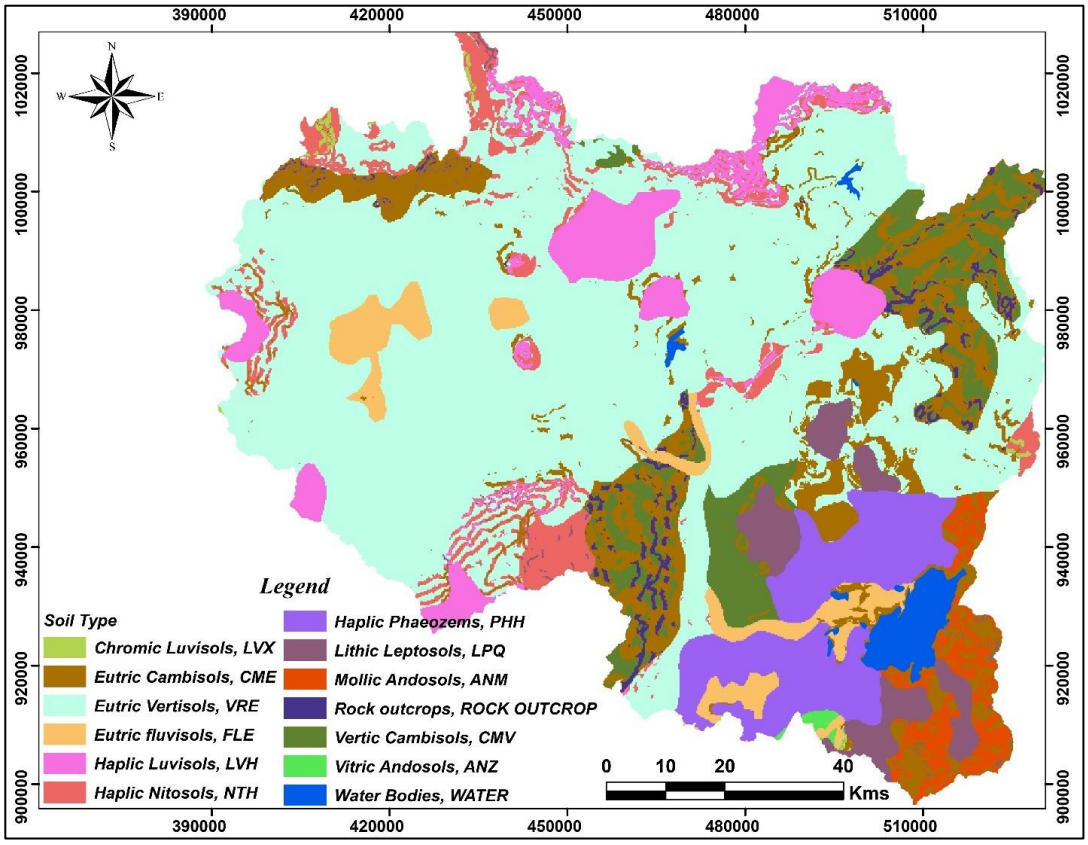

Figure 5: Soil-distributed map.

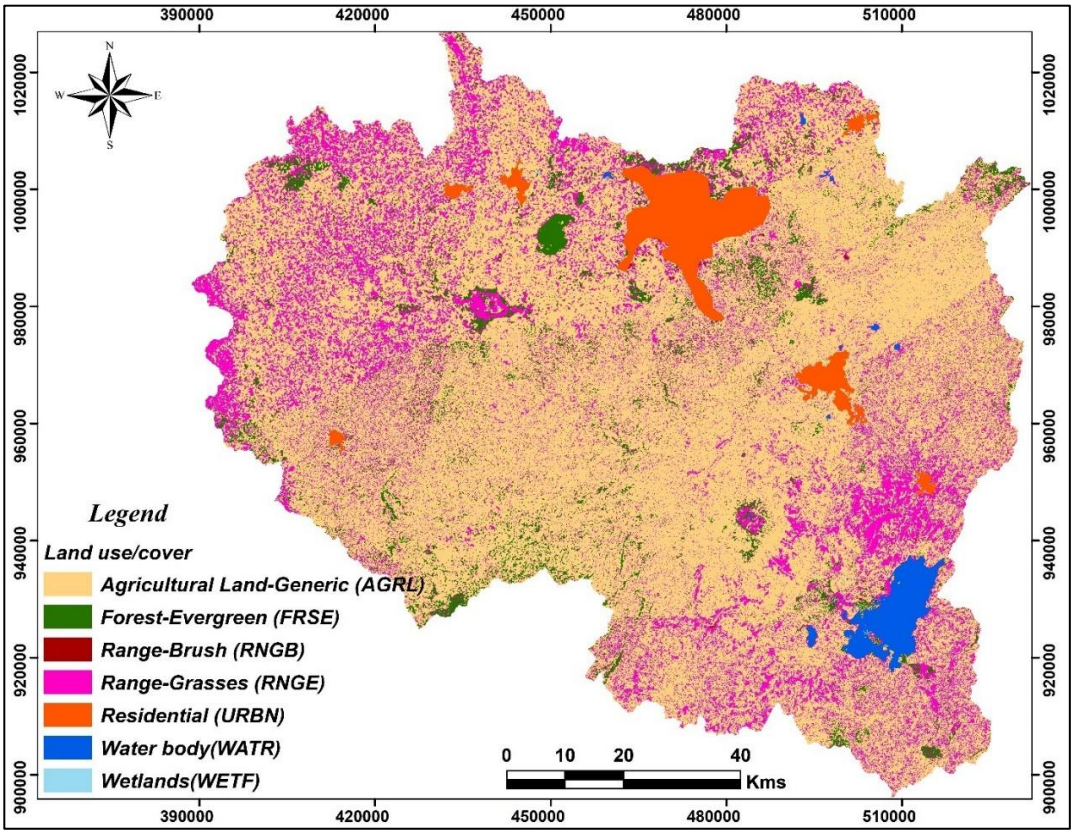

Figure 6: Land use/ cover map (Ethiopian land cover map 2013).

The model setup and simulations were conducted using the ArcSWAT interface integrated with ArcGIS, enabling the use of spatial datasets to represent the watershed's heterogeneity [27]. The theoretical framework is described in detail in the SWAT documentation [8, 28].

2.3. Input Parameters

The SWAT model requires spatial and temporal data inputs including topography, land use, soil, and climate. Watershed delineation was performed using a 30 m × 30 m DEM from the SRTM (USGS), selected because of its adequate spatial detail for sub-basin delineation, broad availability, and successful application in previous Ethiopian hydrological studies with elevations ranging from 1579 to 3564 meters. Slopes were mostly gentle, with 72.1% of the basin falling under 0–10% (Fig. **4**), influencing surface runoff and infiltration behavior. These data were collected from various sources and databases, as summarized in Table 1, providing the minimum necessary information for the SWAT model.

The computer simulation was conducted using ArcGIS 10.2.2 ARC SWAT interface, paired with SWAT version 2012 [7]. The physically based SWAT model requires extensive detailed data about the basin to accurately simulate complex hydrological processes. The data necessary for the SWAT model, including the topography, land use, soil quality, and meteorological data, were collected from various sources and databases. Table **1** presents these data and sources.

Table 1: The available data set for setting the SWAT model.

Sn	Spatial Data	Description	Source
1	Digital Elevation Model	30 m×30 m grid DEM has been used to delineate the boundary of the watershed and analyze the drainage patterns of the terrain.	Shuttle Radar Topography Mission (SRTM) of USGS
2	Land use and land cover	Africa Land Use 2013	Ethiopian Map Agency
3	Soils data	The soil data has been obtained from FAO	Ministry of Agriculture, Government of Ethiopia
4	Weather data	All-weather parameters	Ethiopian Meteorological Agency
5	Hydrological data	Gauge data in the study area gauge station	Ministry of Water, Irrigation and Energy, Government of Ethiopia

Land use data from 2013 show that agricultural land covers 69.1% of the basin, followed by rangeland (20.6%), forests (5.4%), and smaller extents of urban areas and water bodies (Fig. **6**). Soil characteristics were derived from the FAO-UNESCO database [29], dominated by Eutric Vertisols (49.8%) and complemented by Nitosols, Cambisols, and Phaeozems (Fig. **5**), which affect infiltration, percolation, and baseflow processes. Table **2** presents the cover area and percentage distribution of the 12 soil groups in the watershed of the study area, providing a detailed understanding of soil composition and distribution. Climate data (rainfall, temperature, wind speed, solar radiation, and relative humidity) were obtained from 19 meteorological stations covering 1986–2013. These inputs were used to simulate the hydrological processes through HRU discretization.

The SWAT simulates water movement using four main storage components: snowpack, soil profile, shallow aquifer, and deep aquifer. Surface runoff was calculated using a modified SCS Curve Number method, peak runoff using a modified Rational Formula [30], evapotranspiration using the Penman–Monteith equation [25], and baseflow through groundwater flow algorithms [26]. Soil moisture dynamics, lateral flow, and percolation were computed across multiple soil layers, and HRUs enabled spatially variable simulations of these processes based on land use, soil, and slope combinations.

2.4. Sensitivity Analysis

Calibration is an important step in optimizing the model parameters to reduce uncertainty in the model outputs. However, it can be challenging to determining which parameters to be calibrated in models with multiple

parameters can be challenging. Sensitivity analysis is a useful tool for identifying and ranking parameters that significantly affect desired model outputs [31].

Table 2: Characteristics of the modelled upper Awash sub-basin.

Parameter	Type/Class	Area (Km^2)	Basin Area (%)
LANDUSE	Agricultural Land Generic (AGRL)	8077	69.09
	Range-Grasses (RNGE)	2408	20.60
	Forest-Evergreen (FRSE)	625	5.35
	Residential (URBN)	394	3.37
	Water body(WATR)	164	1.40
	Range-Brush (RNGB)	15	0.13
	Wetlands(WETF)	8	0.07
SOIL	Haplic Nitosols (NTH)	606	5.13
	Lithic Leptosols (LPQ)	393	3.33
	Chromic Luvisols (LVX)	22	0.19
	Haplic Luvisols (LVH)	796	6.75
	Eutric fluvisols (FLE)	438	3.71
	Vertic Cambisols (CVE)	656	5.56
	Rock outcrops	142	1.20
	Haplic Phaeozems (PHH)	811	6.87
	Vitric Andosols (ANZ)	19	0.16
	Mollic Andosols (ANM)	251	2.13
	Eutric Vertisols (VRE)	5878	49.81
	Eutric Cambisols (CME)	1596	13.53
SLOP (%)	< 5	4804.03	41.1
	5_10	3623.96	31
	10_20	2209.13	18.9
	20_30	621.74	5.32
	> 30	430.43	3.68

The SWAT Calibration and Uncertainty Programs (SWAT-CUP) use the Sequential Uncertainty Fitting Version 2 (SUFI2) technique to assess the sensitivity of SWAT parameters. This process, carried out alongside the calibration procedure, requires the inclusion of SWAT-estimated and-monitored flows. This is necessary because the objective function, which evaluates the success of the model calibration, bases its sensitivity estimates on the fluctuations in these flows.

Equation 1, which provides the values of the parameters obtained by Latin hypercube sampling versus the objective function values, was used to calculate the sensitivity of the parameters [32].

$$g = \alpha + \sum_{i=1}^{m} \beta_i b_i \quad (1)$$

where g is the objective function value; b is a parameter; α is the regression constant; β corresponds to the technical coefficient attached to variable b; and m is the number of parameters.

The variance mean of the goal function calculates the sensitivity by changing each parameter individually, while keeping the other parameters constant. Sensitivity was assessed using t-statistics (t-stat) and p values. A parameter is considered more sensitive when the absolute value of the t-stat is higher and the p-value is smaller [32]. Sensitivity analysis begins by selecting parameters based on the t-stat and p-value. Following this analysis, the model calibration was performed using the parameters identified as the most sensitive. These parameters are listed in Table **3** as the final parameters of this study.

Table 3: Parameters considered in the sensitivity analysis.

Parameter Name	Description
CN2	SCS runoff curve number
ESCO	Soil evaporation compensation factor
GWQMN	The threshold depth of water in the shallow aquifer required for return flow to occur (mm H2O)
SOL_AWC	Soil available water storage capacity (mm H2O/mm soil)
GW_REVAP	Groundwater revap coefficient
SOL_Z	Soil depth (mm)
SURLAG	Surface runoff lag coefficient (days)
SOL_K	Soil conductivity (mm/h)
CH_K2	Effective hydraulic conductivity in the main channel (mm/h)
ALPHA_BF	Baseflow alpha-factor (days)
GW_DELAY	Groundwater delay (days)
REVAPMN	Threshold depth of water in the shallow aquifer for “revamp” to occur (mm)
CH_K2	Effective hydraulic conductivity in main channel alluvium (mm/hr)
OV_N	Manning’s n value for overland flow
CH_N2	Manning’s coefficient for channels
BIOMIX	Biological mixing efficiency

t-stat was calculated by dividing the regression coefficient of a parameter by its standard error. A parameter is deemed sensitive if its coefficient value exceeds its standard error and the t-stat is greater than zero [33]. The p-value was calculated by comparing the t-stat to the values in the student’s t-test distribution table, testing the null hypothesis that the regression coefficient equals zero.

The analysis used variables that affect the water output of a river basin, which can be modified. These parameters are listed in the SWAT database, including their value ranges, action plans (basin, sub-basin, or HRU), type of value variation (specific value replacement, addition to the existing parameter value, or multiplication of an existing parameter value), and sensitivity analysis groups (water production, sediment yield, or water quality).

2.5. Uncertainty Analysis

Hydrological modeling necessitates an uncertainty analysis to quantify and understand the uncertainties inherent in model predictions. This analysis primarily involves the r-factor and p-factor, which reveal uncertainties in peak flows and volume predictions, respectively.

The r-factor is the ratio of the simulated to the observed flow volume, which assesses the uncertainty associated with the magnitude of the flow predictions. A low r-factor signifies good agreement between the simulated and observed volumes, indicating lower uncertainty. Conversely, a high r-factor indicates a significant discrepancy between the simulated and observed volumes, suggesting higher uncertainty in the model predictions.

In contrast, the p-factor is the ratio of the simulated to the observed peak flows. It evaluates the uncertainty associated with the timing of the peak flows. Similar to the r-factor, a low p-factor denotes good agreement between the simulated and observed peak flows, suggesting lower uncertainty. However, a high p-factor indicates a significant discrepancy in the timing of the peak flows, implying higher uncertainty in the model predictions.

Our evaluation of the reliability and accuracy of hydrological models entails an analysis of these factors in uncertainty analysis. The r and p factors are instrumental in identifying potential sources of uncertainty by measuring the agreement between the observed and simulated flow characteristics.

2.6. Model Calibration and Validation

The first step in calibrating the watershed model involved splitting the measured streamflow time series into two segments: calibration and validation. The calibration period (1988 – 2008) involved adjusting the model inputs, such as rainfall, land use, and soil characteristics, to ensure that the simulated streamflow matched the observed flow at the basin outlet. This iterative process fine-tunes the model parameters to reflect the hydrological conditions of the basin. Once calibration was complete, the model was tested during the validation period (2009 – 2013) using the same input parameters without further adjustments. The purpose of this study was to evaluate the ability of the model to accurately predict streamflow for periods beyond the calibration phase, ensuring that it is robust and reliable for simulating future hydrological scenarios. The predictive capability of the model was assessed by maintaining consistent parameters during validation and determining its effectiveness in representing the watershed's hydrological processes over time.

2.7. Model Performance Evaluation

To assess the behavior of the model, p and r factors were utilized to estimate the uncertainty performance. The p-factor represents the proportion of data covered by the 95PPU (with a maximum value of 100%), whereas the r-factor signifies the average width of the band divided by the standard deviation of the corresponding measured variable. To assess the effectiveness of the model during calibration and validation, we used widely accepted statistical metrics: coefficient of determination (R^2), Nash–Sutcliffe Efficiency (NSE), and Percent Bias (PBIAS). The performance thresholds are based on the guidelines proposed in [34]. According to these criteria, the model performance is rated as "very good" when R^2 and NSE are greater than 0.75, and PBIAS is less than ±10%. A "good" performance corresponds to $0.60 < R^2$ and NSE < 0.75 and ±10% < PBIAS < ±15%. These standards are well suited for evaluating hydrological models and were used consistently in this study to interpret the simulation results at the Hombele and Melkakuntro gauging stations. The coefficient of determination (R^2) illustrates the percentage of variation in the model in the measured data, indicating the magnitude of the linear relationship between the simulated and observed values. Higher numbers suggest less error variance, with values larger than 0.6 generally considered acceptable. R^2 ranges from 0, indicating a poor model, to 1, indicating a good model [35]. Equation 2 can be used to determine the R^2 value:

$$R^2 = \left[\frac{\sum_{i=1}^{n}(O_i - S_i)(S_i - \bar{S})}{\left(\sum_{i=1}^{n}(O_i - \bar{O})^{0.5}\right)\left(\sum_{i=1}^{n}(S_i - \bar{S})^2\right)^{0.5}}\right]^2 \quad (2)$$

Where, O_i – measured value (m3/s)

$\bar{O}$ is the verage measured value (m3/s).

S_i: simulated value (m3/s), and

$\bar{S}$ – Average simulated value (m3/s)

The Nash Sutcliffe efficiency (NSE), a normalized statistic that assesses the amount of residual variation (additionally recognized as "noise") there is about the variance of the measured data (also known as "information") [36] . The NSE represents how well the 1:1 line fits the observed versus simulated data plot. The NSE was calculated using Equation 3:

$$NSE = 1 - \left[\frac{\sum_{i=1}^{n}(OO_{ii} - S_I)^2}{\sum_{I=1}^{n}(O_I - \overline{Oi})^2}\right] \quad 3$$

NSE has a value between negative infinity and one (best), or [-, 1]. An NSE value of 0 denotes poor performance, because it indicates that the mean observed value is a better predictor than the simulated value. When NSE values are greater than 0.5, the simulated value is a better predictor than the mean measured value, and is generally viewed as an acceptable performance [35].

The average tendency of the simulated data to be greater or smaller than their observed equivalents is represented by percentage bias [37]. The low-magnitude values of PBIAS indicate an accurate model simulation, with 0.0 being the ideal value. Positive values denote bias in the model's underestimation, whereas negative values denote bias in the model's overestimation [37]. Equation 4, PBIAS, is calculated as follows:

$$PBIAS = \left[\frac{\sum_{n=1}^{n}(O_I - S_i) * 100}{\sum_{ii=1}^{n}(O_i)}\right] \quad 4$$

Where PBIAS is the deviation of data being evaluated, expressed as a percentage.

2.8. Water Budget Components and Water Yield

In the SWAT model, the components of the water budget are critical drivers of watershed processes that influence everything from plant growth to the movement of sediments, nutrients, pesticides, and pathogens [38]. Watersheds in the SWAT model were divided into sub-watersheds, which were further subdivided into hydrologic response units (HRUs). Each HRU is defined by consistent land-use, slope, and soil characteristics [28]. The SWAT model simulates the hydrological cycle using water budget equation 5 to track these processes across different spatial scales [28].

$$SW_t = SW_O + \sum_{i=1}^{t}\left(R_{day} - Q_{surf} - E_a - S_{Seep} - Q_{gw}\right) \quad 5$$

where SWt is the final soil water content (mm); SWo is the initial soil water content on day i (mm); t is the time (days); R_{day} is the measure of precipitation on day i (mm); Qsurf is the measure of surface runoff on day i (mm); Ea is the amount of ET on day i (mm); W_{seep} is the measure of water entering the vadose zone from the soil profile on day i (mm); and Qgw is the measure of groundwater discharge on day i (mm).

The simulated annual water budget components represent different water inputs and outputs in a specific area over a year. These components include precipitation, evapotranspiration, surface runoff, infiltration, and groundwater recharge. Analyzing the ratio of rainfall to each of these components helps to provide a clearer understanding of the distribution and utilization of water within the area. For example, it reveals how much precipitation is consumed by vegetation, lost through evaporation, and contributes to surface runoff and groundwater recharge. A high ratio of rainfall to evapotranspiration could indicate a densely vegetated area where much of the precipitation is used by plants. Conversely, a low ratio of rainfall to runoff might suggest drought conditions where little precipitation reaches rivers or surface water bodies.

2.8.1. Surface Runoff

The Soil and Water Assessment Tool (SWAT) uses a modified Soil Conservation Service-Curve Number (SCS-CN) [39] to quantify surface runoff. This popular technique combines important hydrological components, making it a reliable method for calculating the runoff in various environments. Daily precipitation data input is the first step in the process and is the main source of information used to estimate the surface runoff. Next, for every sub-basin or Hydrologic Response Unit (HRU) in the watershed, SWAT designates a Curve Number (CN). The CN value, which ranged from 30 to 100, was determined based on the soil type, antecedent moisture conditions (AMC), and land use. A lower CN denotes higher infiltration and a reduced potential for runoff, whereas a larger CN suggests a higher potential for runoff.

Before calculating the runoff, SWAT accounts for the initial abstraction (I_a), which includes water loss due to infiltration, evaporation, and storage in surface depressions. This initial abstraction was calculated as a fraction of

the potential maximum retention (S), using the relationship I_a = 0.2S. The maximum potential retention was determined using Equation 6:

$$S = \frac{1000}{CN} - 10 \quad (6)$$

Where S represents the amount of rainfall retained by the soil before runoff is generated. Using these parameters, SWAT calculates the surface runoff (Q) using Equation 7:

$$Q = \frac{(P-I_a)^2}{(P-I_a)+S} \quad (7)$$

Where P is the total rainfall, and I_a is the initial abstraction. This approach allows SWAT to accurately simulate surface runoff by accounting for various landscape characteristics and hydrological processes, making it a powerful tool for water resource management and planning in complex watershed systems.

2.8.2. Evapotranspiration

Evapotranspiration, the combined process of water loss through evaporation from soil and water surfaces and transpiration from plants, is a critical component of the water balance and a key factor in the hydrological cycle. However, the accurate estimation of evapotranspiration is challenging and often involves a degree of uncertainty. In the SWAT model, evapotranspiration was calculated using the FAO Penman-Monteith method (FAO56PM), a widely accepted approach developed by [40]. This method estimates the reference crop evapotranspiration (ET), which represents the rate of evapotranspiration from a well-watered reference crop, such as grass or alfalfa, under standard environmental conditions.

The FAO56PM model incorporates various climatic factors such as temperature, humidity, solar radiation, and wind speed to calculate ET. The Equation 8:

$$ET = \frac{0.408\Delta(R_n-G)+\gamma\frac{900}{T_a+273}u_2(e_s-e_a)}{\Delta+\gamma(1+0.34u_2)} \quad (8)$$

Where ET is the reference crop evapotranspiration (mm/d), γ is the psychrometric constant (kPa/°C), Rn is the net solar radiation at the crop surface (MJ/m2/d), G is the soil heat flux (MJ/m2/d), Δ is the slope of the saturation vapor pressure versus air temperature curve (kPa/°C), Ta is the mean air temperature at a 2m height (°C), u2 is the wind speed at a 2m height (m/s), es is the saturation vapor pressure (kPa), and ea is the actual vapor pressure (kPa).

In SWAT, the calculated reference evapotranspiration is used along with the soil and plant characteristics to estimate the actual evapotranspiration across the watershed. The model calculates the annual water budget in each cell by considering the runoff and actual evapotranspiration. To simplify the calculations, percolation and deep percolation components are often not separately accounted for in the water budget of the model. This approach ensures a comprehensive understanding of water loss through evapotranspiration, thereby aiding in the accurate simulation of hydrological processes.

2.8.3. Groundwater Recharge

Groundwater recharge is an essential process in the water cycle, providing a consistent supply of water for various uses. The groundwater recharge in the SWAT model was calculated by modeling the flow of water from the surface through the soil and vadose zone to the water table, where it contributes to the aquifer. This flow is affected by various factors, including topography, soil properties, and the characteristics of the vadose zone, which is the area between the ground surface and water table that influences the downward movement of water [38]. The SWAT model uses an exponential decay function, originally proposed by [41] to estimate the groundwater recharge. According to this function, as water infiltrates deeper from the surface, the recharge rate decreases exponentially because of lower hydraulic conductivity and increased resistance to water flow. This relationship is particularly effective in areas where the vadose zone is relatively uniform, allowing the model to predict the groundwater recharge more accurately. The exponential decay function is expressed in Equation 9.

$$R_z = R_o e^{-\alpha z} \quad (9)$$

Where R_z is the recharge rate at depth z, Ro is the recharge rate at the surface, α is a decay constant that depends on the hydraulic properties of the soil and the vadose zone, and z is the depth below the surface. This equation accounts for the hydraulic properties of the soil, including porosity, permeability, and depth to the water table, all of which influence how quickly the water reaches the aquifer. By incorporating land cover and climatic data, the SWAT uses this function to model the volume of water moving from the soil layers into the groundwater system.

2.8.4. Total Water Yield

Water yield is a key parameter for sustainable water resource management in the study area. Water yield refers to the total volume of water exiting a hydrologic response unit (HRU) and flowing into the main channel during each time step of the simulation [28]. This metric is crucial, as it provides insight into the available water resources within a watershed, aiding in the planning and allocation of water for various uses, such as agriculture, industry, and ecosystem services. The SWAT model evaluates water yield within a watershed based on the calculations outlined in Equation 10. This equation captures the interactions among precipitation, evapotranspiration, surface runoff, and other hydrological processes, allowing for a comprehensive understanding of water availability at different spatial and temporal scales.

$$W_{yld} = Q_{surf} + Q_{gw} + Q_{lat} - T_{loss} \quad (10)$$

Where W_{yld} represents the water yield (mm), which is the total water output from the hydrologic response unit (HRU). Q_{surf}: Surface runoff (mm), which is the portion of water flowing directly over the land surface into the stream. Q_{lat}: Lateral flow (mm), indicating subsurface flow that moves horizontally through the soil and contributes to the streamflow. Q_{gw} the groundwater flow (mm), which refers to water entering the stream from the groundwater system. T_{loss}: Transmission loss (mm), representing the water lost from the tributary as it infiltrates the streambed.

3. Results and Discussion

3.1. Watershed Delineation

The watershed was segmented into 35 sub-basins using topographic and stream network analysis. Hombele (sub-basin 33) and Melkakuntro (sub-basin 20) were selected based on data availability, representativeness of the upper and lower watershed hydrology, and completeness of streamflow records. This segmentation is based on a digital elevation model (DEM) and stream network. Within each of these sub-basins, the SWAT model further subdivided the landscape into 1,415 hydrological response units (HRUs). These HRUs were differentiated based on variations in land use, soil type, and slope gradient. This methodology facilitated a more precise representation of spatial variability within the study area. Notably, the fluviometric station of Hombele was positioned in sub-basin number 33, and Melkakuntro was located in sub-basin number 20.

3.2. Sensitivity Analysis

The sensitivity analysis conducted in this study initially considered 16 parameters to identify the most influential factors affecting the streamflow in the study area. After analyzing the results, six parameters were found to have the lowest p-values and highest t-stat values, indicating their sensitivity to streamflow at both monitoring stations. The first parameter identified was the SCS runoff curve number (CN2), which represents the ability of soil to absorb water. This parameter is a critical factor for determining the amount of runoff generated during rainfall events. The second parameter, the alpha factor (ALPHA_BF), was largely responsible for the groundwater recharge rate. It measures the rate of water transfer from the surface to groundwater system. The third parameter, groundwater delay (GW_DELAY), represents the time required for the water to move from the surface to the groundwater system. This parameter is crucial for determining when and how quickly the groundwater recharges. The fourth parameter is the threshold depth of water in the shallow aquifer necessary for

return flow to occur (GWQMN). This denotes the minimum amount of water required in the shallow aquifer for water to return to the surface, as shown in Fig. (**7**) and (**8**).

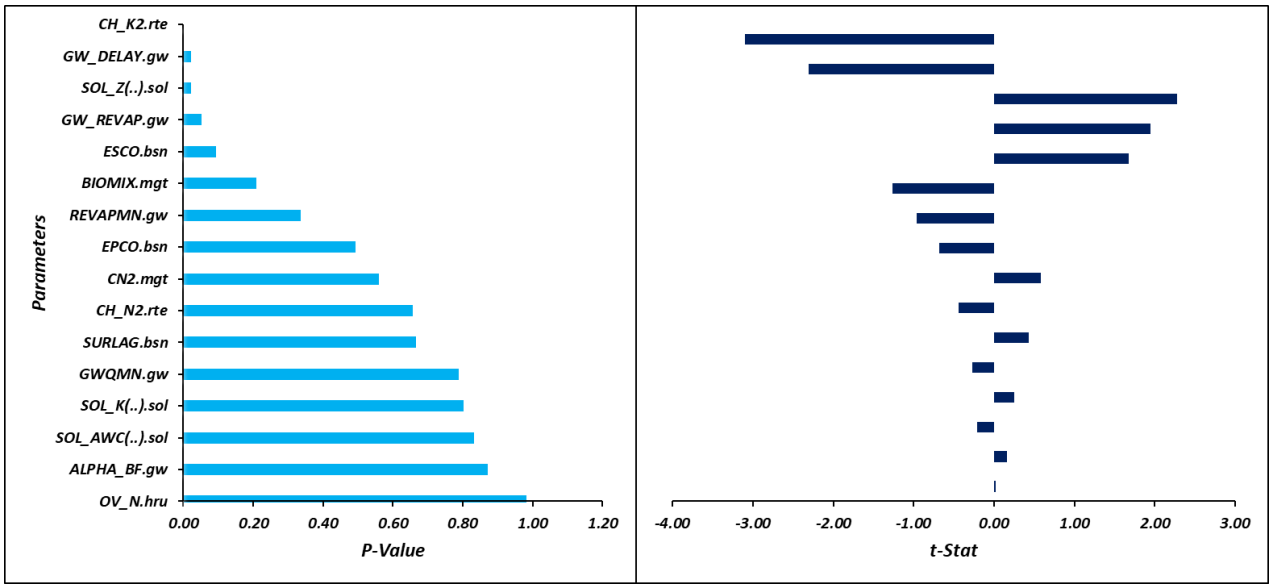

Figure 7: Sensitivity of flow parameters Hombele gauging station.

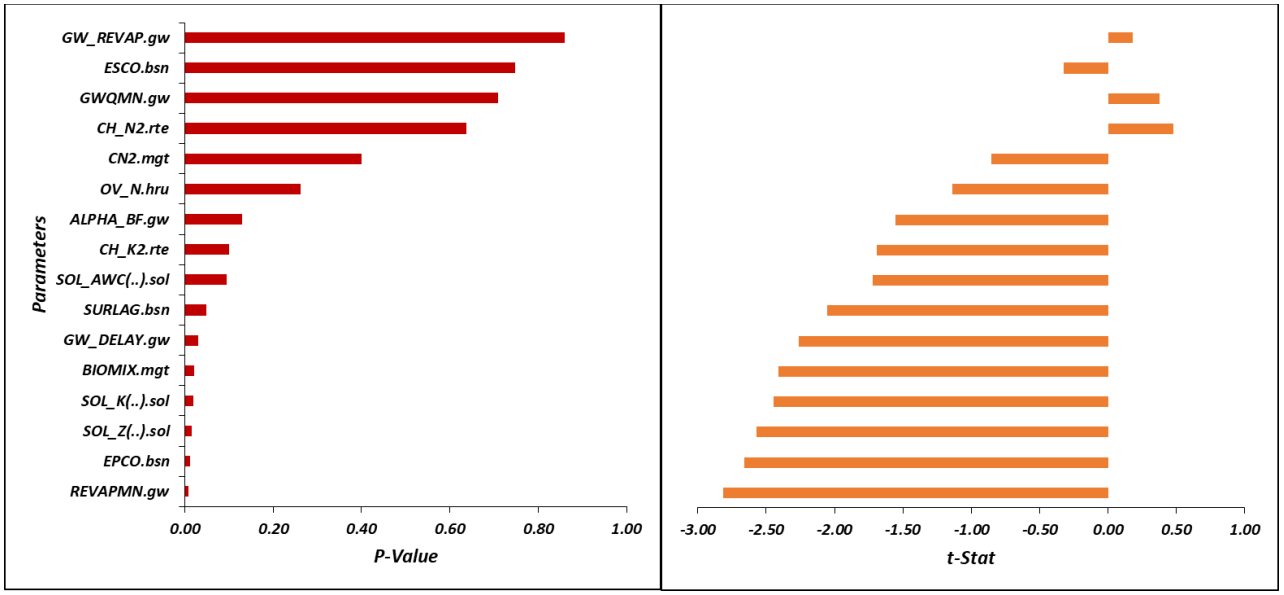

Figure 8: Sensitivity of flow parameters at Melkakuntiro gauging station.

3.3. Calibration, Validation, and Uncertainty Analysis

Table **4** presents the initial ranges and calibrated sensitive parameters for the streamflow in the study area. It provides valuable information on the range of values for each parameter and the final calibrated values after sensitivity analysis. This information is crucial for understanding the factors that influence streamflow and developing sustainable water resource management strategies. Plots of daily simulated and observed streamflows were constructed for the gauging stations at Hombele and Melkakuntiro to assess the effectiveness of the calibrated model. The results showed good agreement between the datasets, with Nash Sutcliffe Efficiency (NSE) values of 0.82 and 0.78 and R^2 values of 0.82 and 0.79 for the calibration period (1988–2008), respectively. During the validation period (2009-2013), NSE and R^2 values were 0.67 and 0.66, and 0.71 and 0.7, respectively Fig. (**9**).

Table 4: Initial ranges and final calibrated sensitive parameters.

Parameter	Minimum	Maximum	Calibrated Value
Alpha_Bf	0	1	0.048
Biomix	0	1	0.2
Ch_K2	0	150	0
Ch_N2	0	1	0.014
Cn2	35	98	71.2
Epco	0	1	1
Esco	0	1	0.95
Gw_Delay	0	50	31
Gw_Revap	0.02	0.2	0.02
Gwqmn	0	5000	1000
Revapmn	0	500	750
Sol_Awc	0	1	0.1
Sol_K	0	100	17.27
Sol_Z	0	3000	204.03
SURLAG	0	10	4
OV_N	0	0.8	0.14

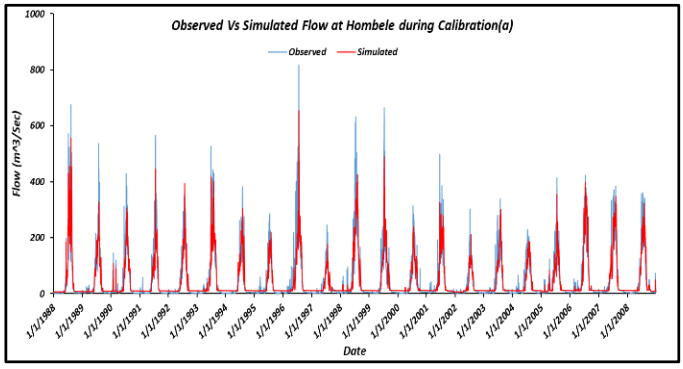

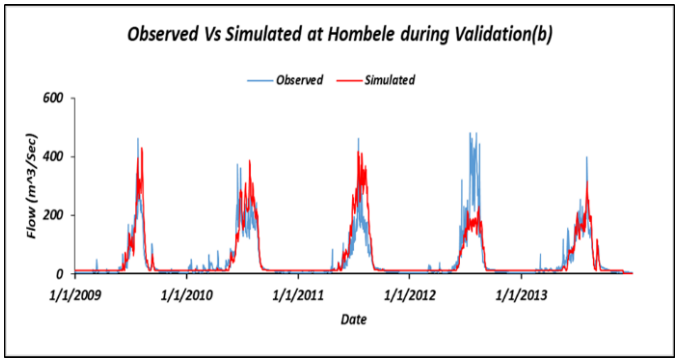

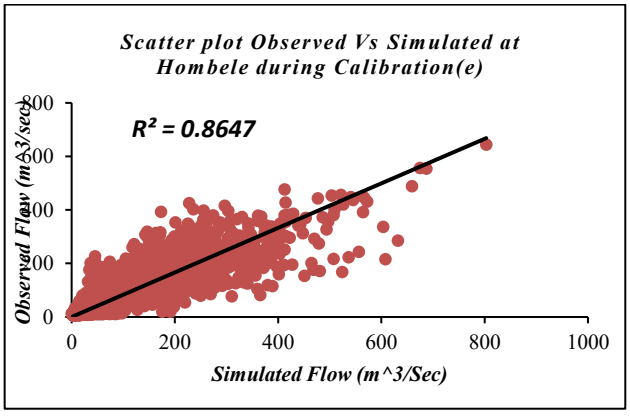

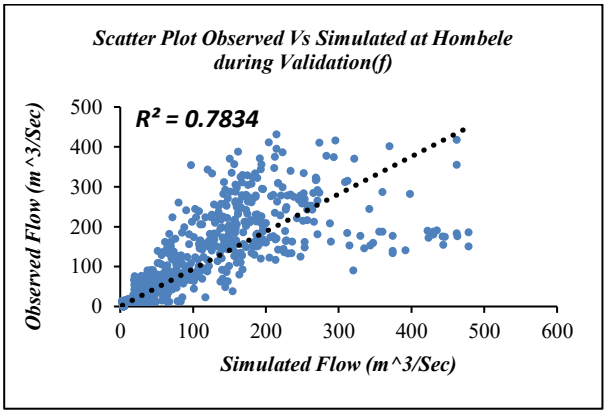

Fig. 9: contd....

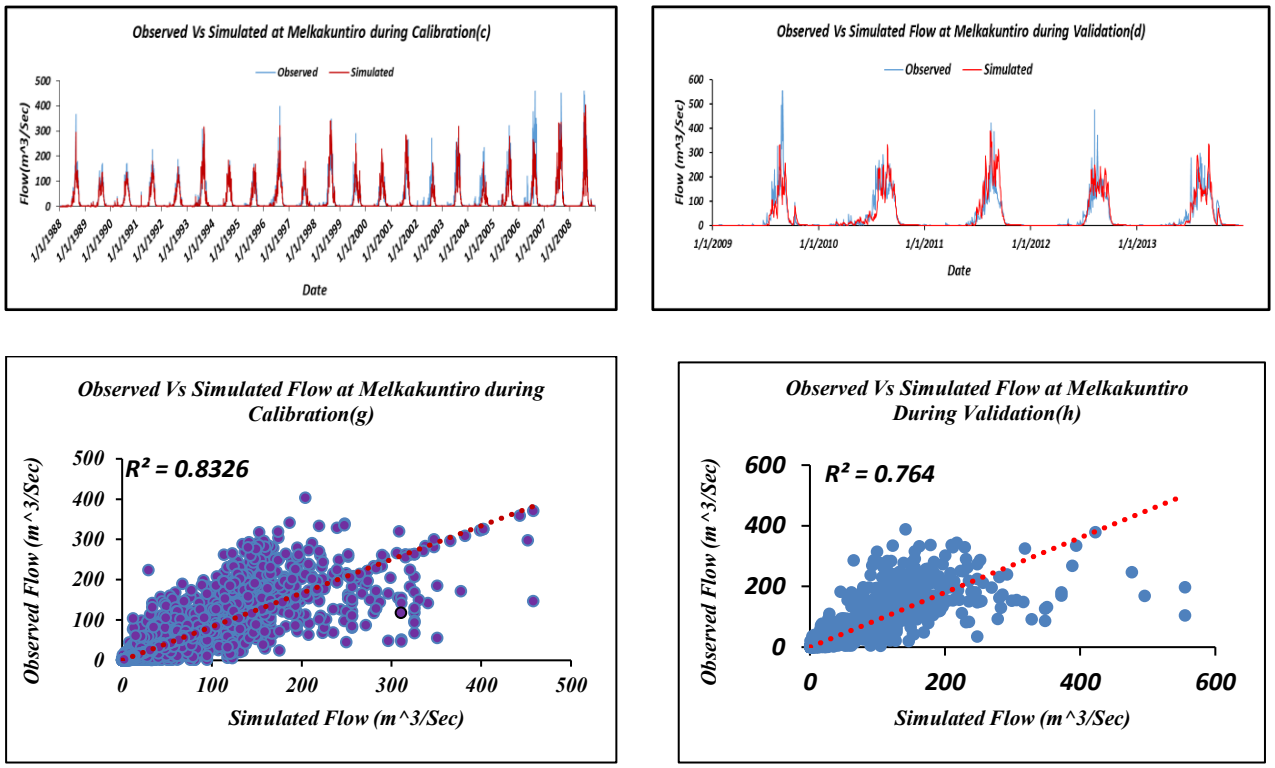

Figure 9: The time series data for Hombele (**a** & **b**) and Melkakuntiro (**c** & **d**) are depicted for both the calibration and validation period and scatter plots illustrate the comparisons of daily streamflow between simulated and observed data at Hombele (**e** & **f**) and Melkakuntiro (**g** & **h**) during the calibration and validation processes.

Considering the model performance statistics for the calibration periods at Hombele and Melkakuntro stations, and based on the criteria set out by Moriasi *et al*. for assessing model performance, the setup model was rated as "very good" and "good" respectively shown in Table **5**. For the validation period, the ratings were "good." These model performance measures indicate that the model accurately captured the observed streamflow at Hombele station. However, a comparison of the statistical measures for the calibration and validation periods revealed that the model performed better during the calibration period than the validation period.

Table 5: Classification of statistical indices.

R^2	NSE	PBIAS	Classification
$0.75 < R^2 < 1.00$	$0.75 < NSE < 1.00$	PBIAS < ± 10	Very Good
$0.60 < R^2 < 0.75$	$0.60 < NSE < 0.75$	+ 10 < PBIAS < + 15	Good
$0.50 < R^2 < 0.60$	$0.36 < NSE < 0.60$	+ 15 < PBIAS < + 25	Satisfactory
$0.60 < R^2 < 0.50$	$0.00 < NSE < 0.36$	+ 25 < PBIAS < + 50	Bad
$R^2 < 0.25$	NSE < 0.00	+ 50 < PBIAS	Inappropriate

Source: Adapted from Moriasi *et al*. [34],

The observed and simulated discharges matched well during the calibration and validation periods Table **6**. However, during the calibration period at the Hombele and Melkakuntro gauging stations, the average underestimations of the observed discharge were 2.3% and 13.1%, respectively. During the validation period, the observed discharge was overestimated by 11.2% and 1.9% in Hombele and Melkakuntro, respectively. During the calibration period (1988–2008), the observed and simulated mean annual flow (MAF) were 1421 MCM/yr (45.03 m3/s) and 1389 MCM/yr (44.01 m3/s), respectively, indicating an underestimation of the observed streamflow by

2.3% at the Hombele station. The observed and simulated MAF at Melkakuntro were 943 MCM/yr (29.88 m3/s) and 819 MCM/yr (25.96 m3/s), respectively, representing a 13.1% underestimation of the observed streamflow. For the validation period (2009-2013), the observed and simulated flows (MAF) at Hombele and Melkakuntro were 1450 MCM/yr (45.95 m3/s), 1612 MCM/yr (51.08 m3/s), 1140 MCM/yr (36.13 m3/s), and 1160 MCM/yr (36.8 m3/s), respectively, resulting in an overestimation of the observed discharge by 11.2% and 1.9%.

Table 6: Performance indexes.

Performance Indexes	Gauging stations			
	Hombele		Melkakuntro	
	Calibration	Validation	Calibration	Validation
R^2	0.82	0.71	0.79	0.7
NSE	0.82	0.63	0.63	0.66
PBIAS	2.3	-11.2	13.1	-1.9

For Hombele, the p- and r-factor ratios during calibration were 0.801 and 0.97, respectively. This indicates that the model was able to reasonably simulate the peak flow and volume of flow, capturing approximately 80.1% and 97% of the observed values, respectively. Similarly, for Melkakuntro, the p- and r-factor ratios during calibration were 0.808 and 0.868, respectively, indicating a slightly lower but still acceptable level of performance, as shown in Table **7**.

Table 7: Uncertainty indexes.

Uncertainty Indexes	Gauging stations			
	Hombele		Melkakuntro	
	Calibration	Validation	Calibration	Validation
p-factor	0.801	0.387	0.808	0.352
r-factor	0.97	0.9	0.868	0.98

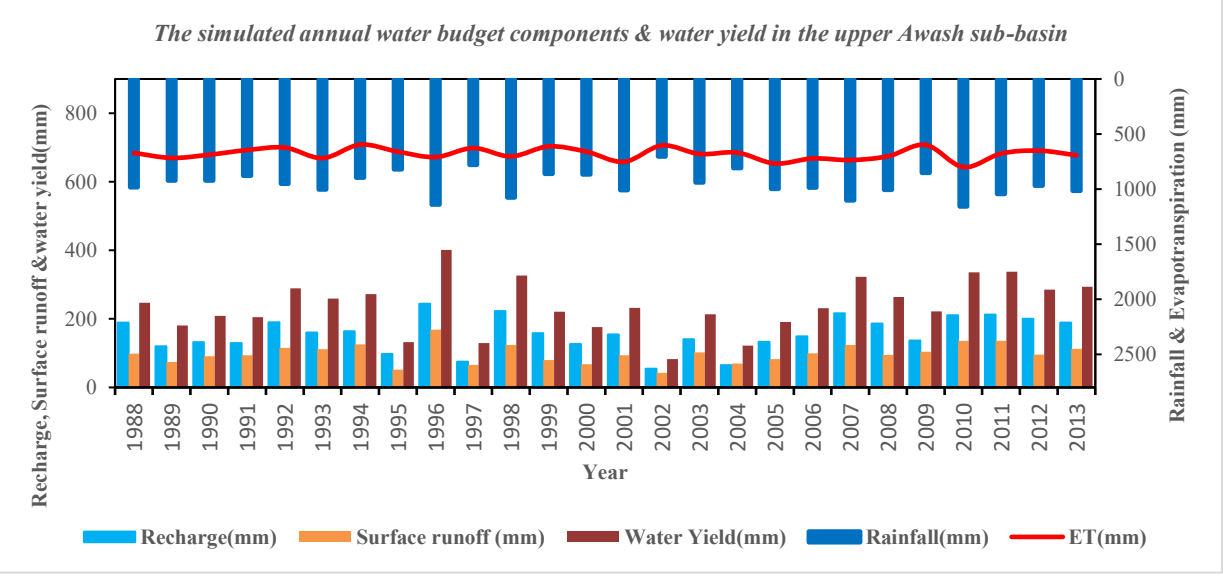

Figure 10: The simulated annual water budget components and water yield in the upper Awash sub-basin.

3.4. Water Budget Components and Water Yield in the Upper Awash Sub-basin

The components of the simulated annual water budget and water yield for the study area are shown in Fig. (**10**). These elements include annual amounts of precipitation, evapotranspiration, surface runoff, and groundwater recharge in the region. The annual rainfall in the study area is shown in Fig. (**11**).

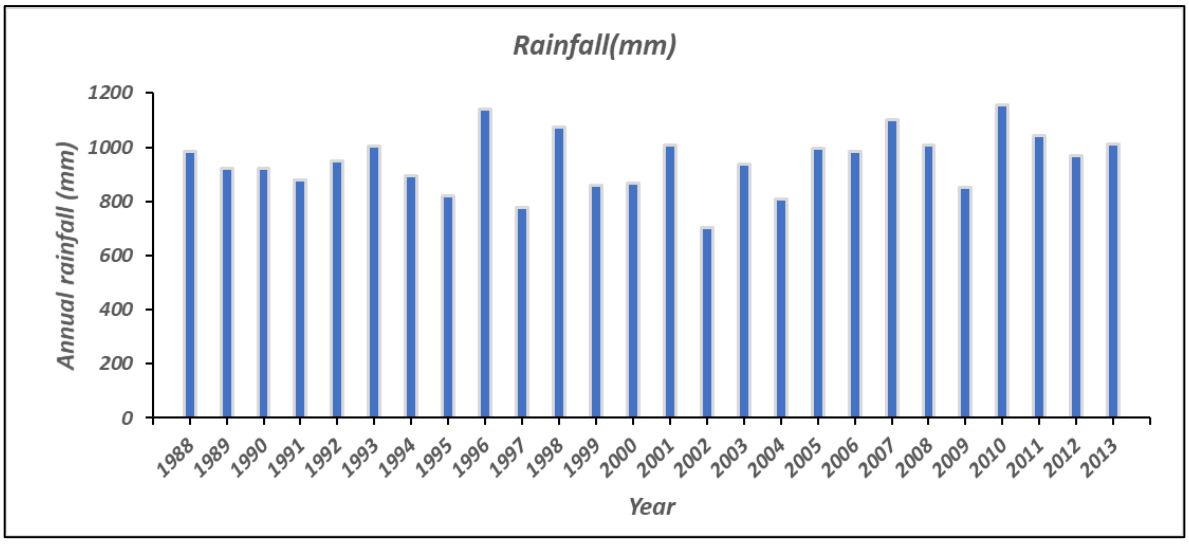

Figure 11: The simulated annual rainfall in the upper Awash sub-basin.

3.4.1. Surface Runoff

Fig. (**12**) shows the annual surface runoff in the study area. According to the data analysis, annual surface runoff in the sub-basin ranges from 0 mm to 240.5 mm, with a mean value of 93.4 mm/year and a standard deviation of 30.1 mm. These numbers reveal the variability in surface runoff and the capacity of the sub-basin to manage its water resources. The mean annual spatial pattern of the surface runoff in the sub-basin is shown in Fig. (**13**). The graph demonstrates that the Hombele area, owns, and cities had the most considerable surface runoff (149.7-240.5 mm).

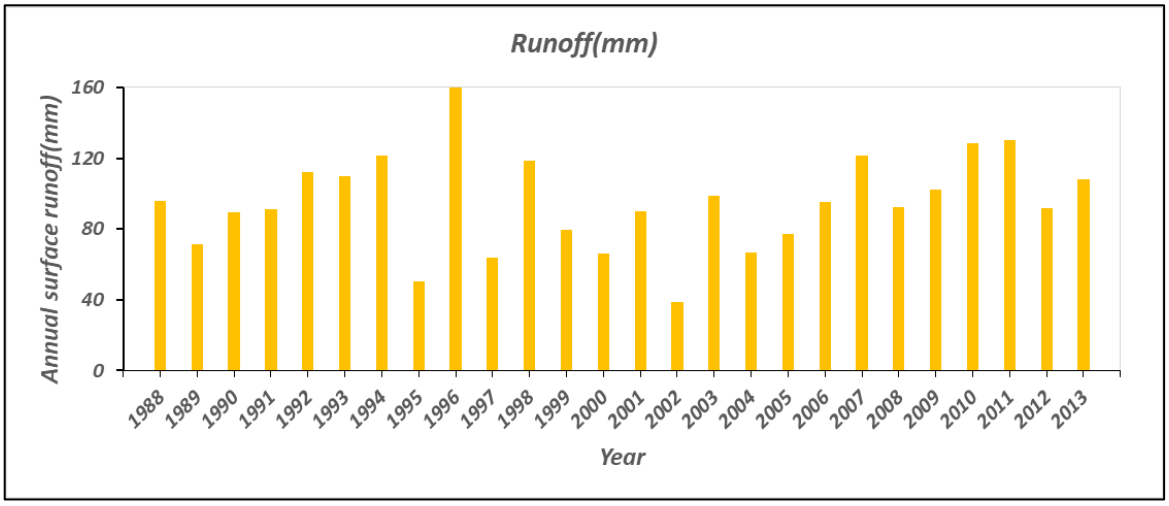

Figure 12: The simulated annual surface runoff in the upper Awash sub-basin.

3.4.2. Evapotranspiration

The annual evapotranspiration in the upper Awash sub-basin ranges from 22.6 mm to 2237.8 mm, demonstrating significant variation. With a standard deviation of 200 mm, the average annual evapotranspiration

in the basin was 682.5 mm. These figures highlight the critical role of evapotranspiration in the region's water budget, accounting for 71.8% of the annual rainfall. This indicates that a substantial portion of rainfall is lost to the atmosphere through evaporation and transpiration, affecting the management of water resources and the supply of water for both human and agricultural use. Fig. (**14**) shows the annual evapotranspiration occurring within the study area. The spatial distribution of mean annual evapotranspiration reveals that open water bodies, such as Koka, Abasamuel, and lakes around Debrezeit, have high evapotranspiration rates, ranging from 1171.1 to 2237.8 mm, as shown in Fig. (**15**).

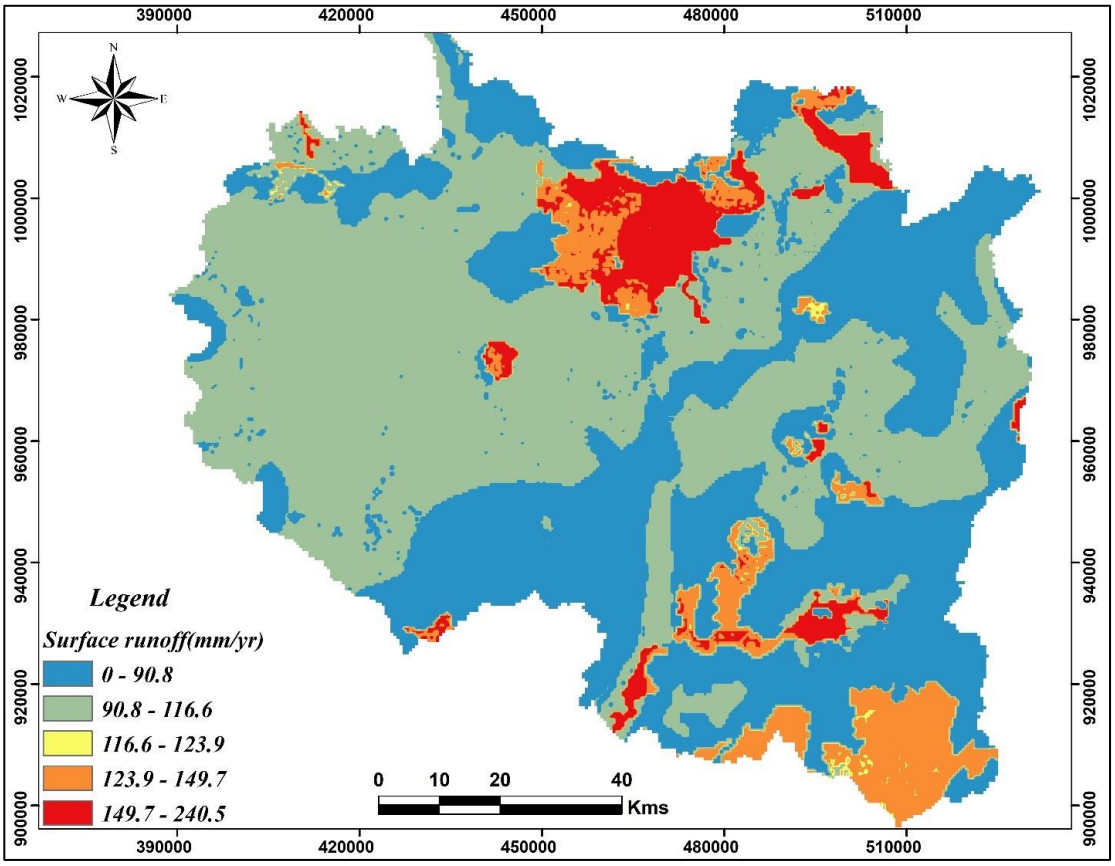

Figure 13: The mean annual spatial distribution of surface runoff.

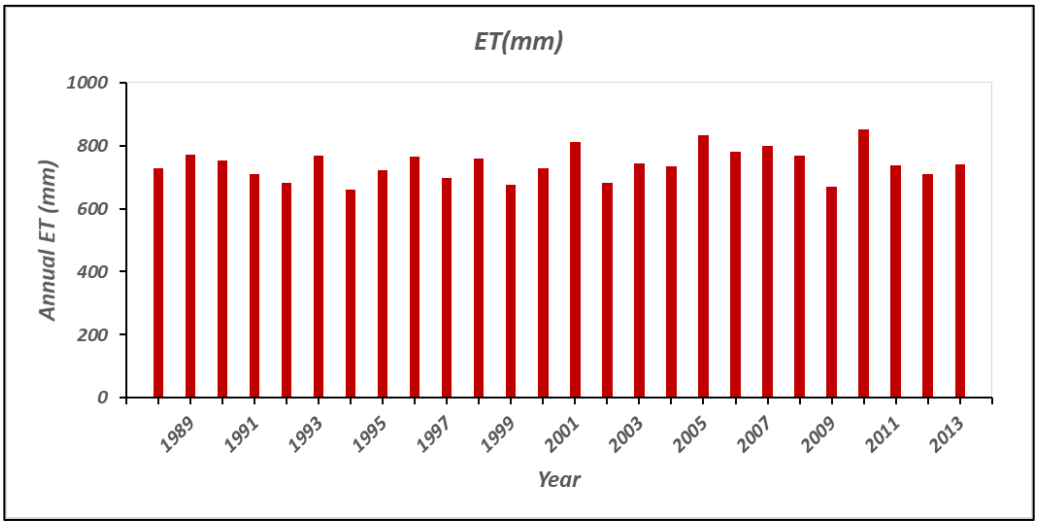

Figure 14: The simulated annual evapotranspiration in the upper Awash sub-basin.

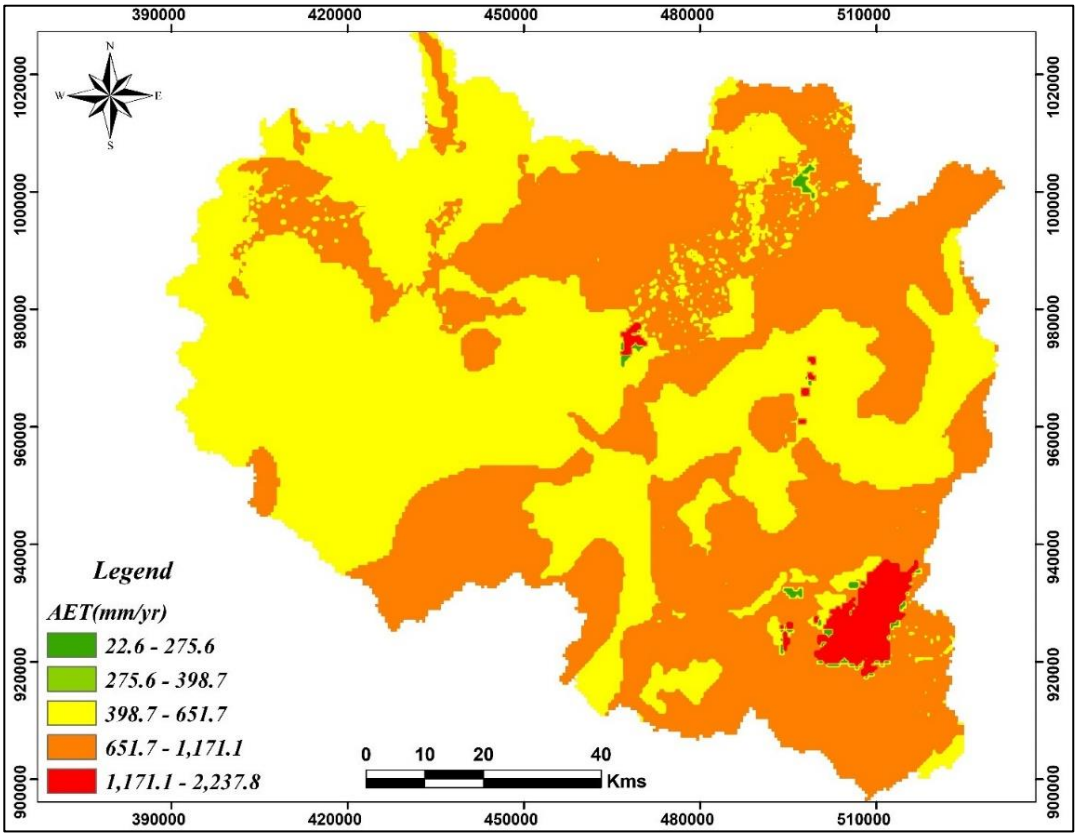

Figure 15: The mean annual spatial distribution of evapotranspiration.

3.4.3. Groundwater Recharge

The bar chart in Fig. (**16**) Shows the annual groundwater recharge in the study area. The annual groundwater recharge in the upper Awash River Basin exhibited significant spatial variation, with values ranging between 0 and 904.3 mm, as depicted in Fig. (**17**). The recharge estimation indicated that the total aquifer recharge for the entire basin, calculated using the long-term (28 years) mean annual recharge, was 181.1 mm/year. This calculation had a standard deviation of 64.9 mm, representing 19.1% of the average annual rainfall. These figures highlight the variability in groundwater recharge in the study area and the potential for long-term groundwater management.

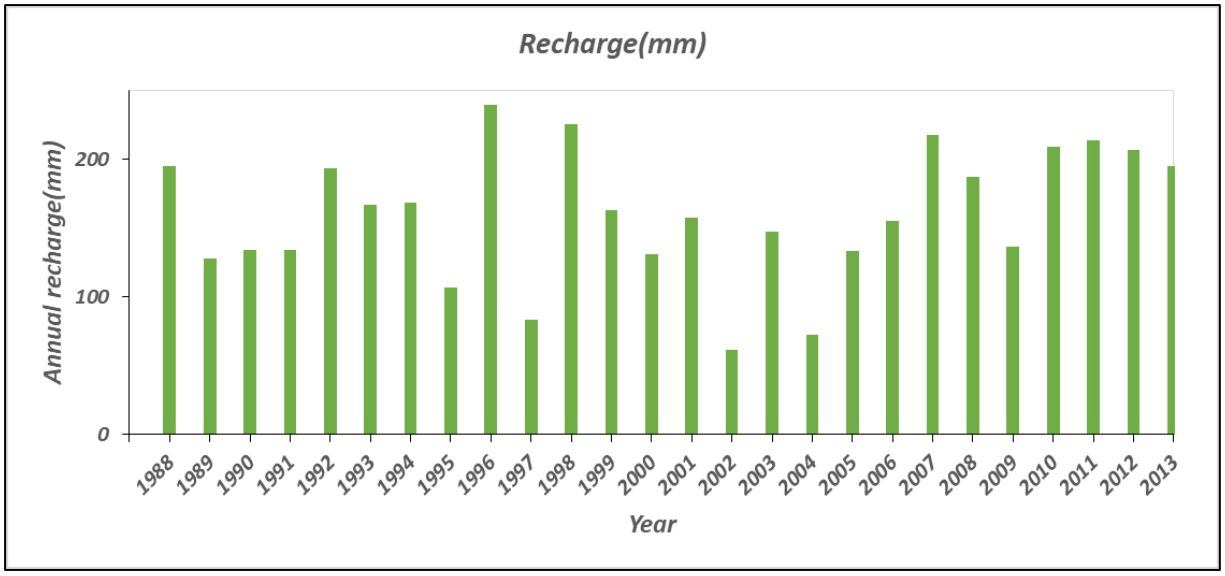

Figure 16: The simulated annual groundwater recharge in the upper Awash sub-basin.

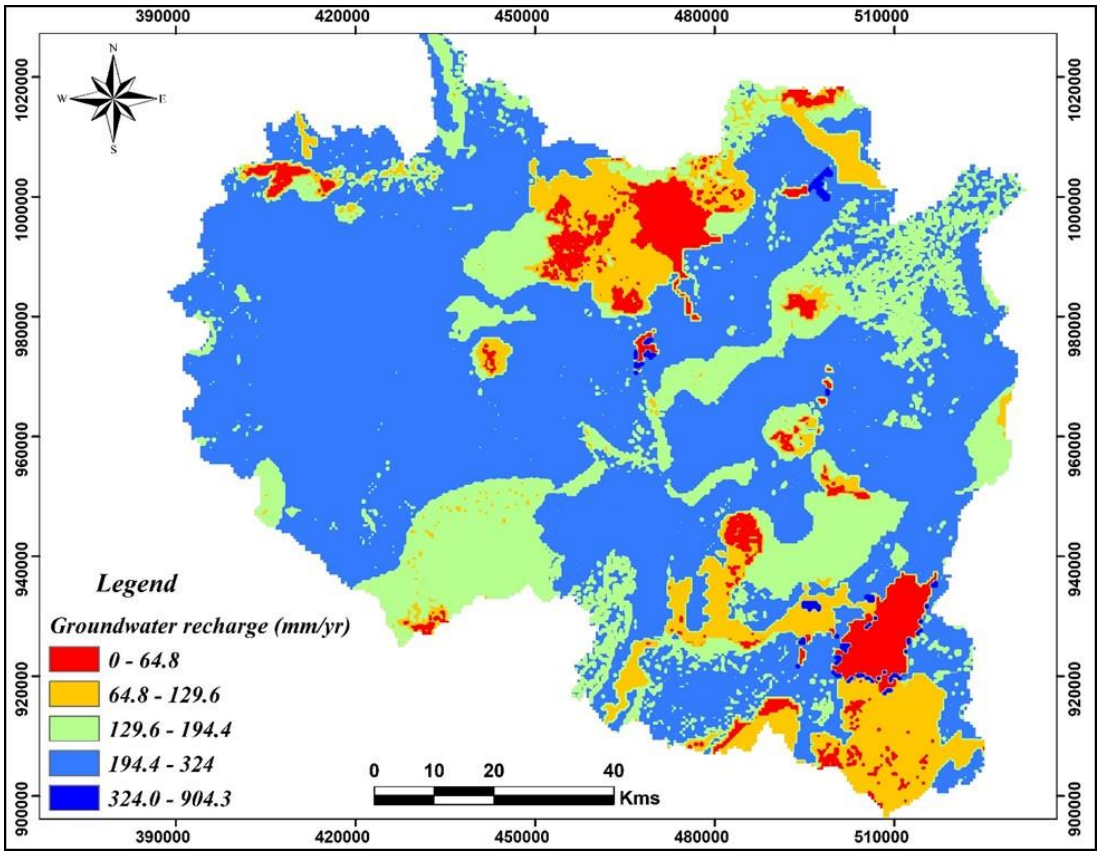

Figure 17: The mean annual spatial distribution of groundwater recharge.

This study found that agricultural land, designated AGRL, exhibited the highest mean annual groundwater recharge value. This conclusion underscores the pivotal role of agricultural regions in sustaining water resources as they significantly contribute to groundwater recharge. In contrast, urban (URBN) land use types were associated with the highest surface runoff values, indicating that urban areas contribute more to runoff than other land use types. Furthermore, land use/cover types encompassing aquatic bodies displayed the highest evapotranspiration values, suggesting that these areas experienced elevated rates of water loss through evaporation and transpiration. Conversely, the land use/cover-type water bodies exhibited the lowest mean annual groundwater recharge and surface runoff values, implying that these areas make limited contributions to groundwater recharge and runoff. In contrast, urban (URBN) land use/cover types demonstrated the lowest evapotranspiration values, indicating that urban areas experience lower rates of water loss through evaporation and transpiration compared to other land use types. Fig. (**18**) visually represents these disparities in the mean annual groundwater recharge, surface runoff, and evapotranspiration values across different land-use types.

3.4.4. Rainfall and its Partitioning

Rainfall is the primary source of water entering watersheds, and is distributed among three key components: groundwater recharge, surface runoff, and evapotranspiration. The ratios of rainfall to groundwater recharge, surface runoff, and evapotranspiration provided critical insights into the hydrological dynamics of the Upper Awash River sub-basin. It is important to understand the ratio range of the constituents of the water budget, as shown in Fig. (**19**).

The predominance of evapotranspiration in the Upper Awash River sub-basin, accounting for 71.8% of the total precipitation, suggests that a large portion of incoming water is lost to the atmosphere. This is common in regions with significant vegetative cover and high temperature. The sub-basin water cycle depends heavily on evapotranspiration, which significantly affects the amount of water available for surface runoff and groundwater recharging. This affects the overall water balance and resource management in the region.

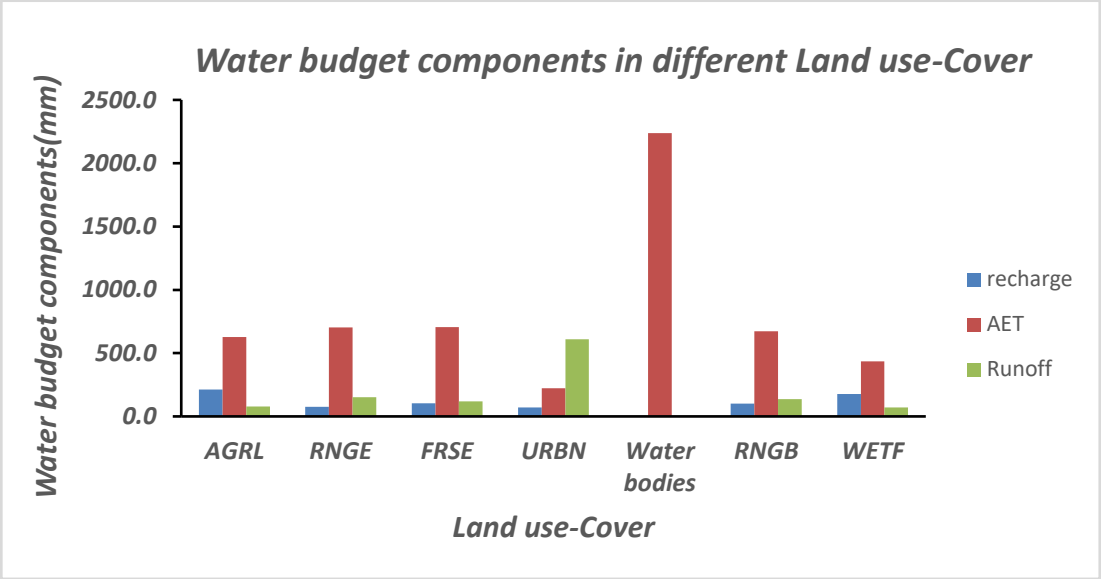

Figure 18: Actual evapotranspiration, recharge, and surface runoff components in different land-cover use units.

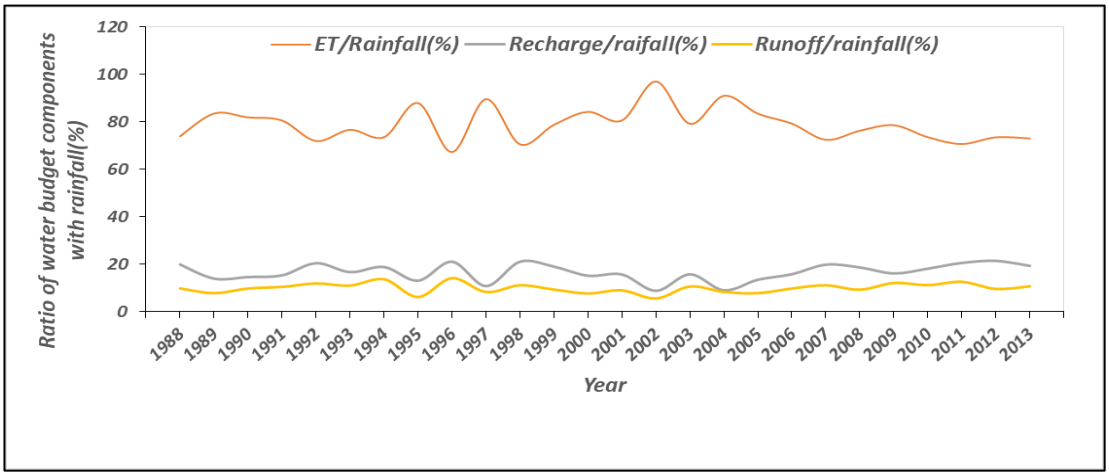

Figure 19: The ratio of rainfall to water budget components in the upper Awash sub-basin.

Aquifer replenishment was moderately aided by groundwater recharge, which accounted for 19.1% of total precipitation. The region's industrial, agricultural, and domestic requirements depend on the groundwater supply that this water fraction helps to maintain. Conversely, the low 9.8% surface runoff ratio indicated that most of the precipitation was either absorbed by the soil or evaporated through evapotranspiration rather than runoff. It can be inferred that the porous soils and vegetation cover of the sub-basin significantly boosted infiltration, thereby reducing direct runoff. However, low surface runoff also makes the management of water resources challenging, particularly under arid or drought conditions. These findings underscore the necessity of implementing integrated approaches to water resource management that consider the vital functions of evapotranspiration and groundwater recharge in maintaining water supplies.

3.4.5. Total Water Yield

In addition to estimating the monthly discharge of the watershed, the SWAT model calculates other key components of the water balance. Water yield is a crucial parameter for effective water management and planning in the study area. The model was used to assess the contribution of each sub-watershed to the overall water yield during the simulation period, utilizing calibrated parameters to provide a detailed analysis of the water distribution across the watershed. This information is essential for understanding the water availability and guiding resource management decisions.

Sub-basin 5, dominated by agricultural land cover, recorded the lowest water yield in the watershed with an estimated 232.3 mm. In contrast, sub-basin 1, characterized by wetland land use, exhibited the highest water yield at 245.9 mm. The variation in water yield across the sub-basins highlights the influence of land-use and land-cover types on hydrological processes within the watershed. The overall average water yield for the study area was 233.4 mm, reflecting the combined effect of different land cover types and hydrological dynamics across the watershed.

A detailed breakdown of the average annual water budget components, including the water yield for each sub-basin, is presented in Table **8**. These data provide valuable insights into the spatial distribution of water availability and help inform decisions for sustainable water management and planning across various land-use types in the watershed.

Table 8: Uncertainty indexes.

Water Budget Components & Water Yield	Depth(mm)
Precipitation	1078
Surface runoff	93.4
Groundwater (Shallow aquifer) flow	165
Till flow	0
Evapotranspiration	682.5
Transmission loss	27.2
Total water yield	233.4

Compared with similar watersheds globally, such as the Kaidu-Kongqi River Basin in arid Northwest China [42] and parts of the volcanic Upper Blue Nile Basin in Ethiopia [14], the water budget components observed in the upper wash sub-basin reflect comparable trends, especially in terms of high evapotranspiration ratios and moderate groundwater recharge. However, the Upper Awash showed lower surface runoff, likely due to its porous volcanic soils and land use characteristics. These insights suggest that water management in the region is moderately sustainable but requires improved conservation practices to address potential scarcity during dry periods.

4. Conclusions and Perspectives

This study successfully employed the Soil and Water Assessment Tool (SWAT) to conduct a detailed analysis of the water budget components within the Upper Awash River sub-basin in Central Ethiopia. Based on a significant quantity of data from 1986 to 2013, the calibration and validation of the model showed strong performance metrics, such as acceptable values for the p-factor, r-factor, NSE, R^2, and PBIAS at two gauging stations: Hombele and Melkakuntro. During the calibration phase, Hombele demonstrated p- and r-factor ratios of 0.801 and 0.97, respectively. This indicated that the model captured approximately 80.1% and 97% of the observed values for the peak flows and flow volume, respectively. In contrast, Melkakuntro had slightly lower, but still acceptable ratios of 0.808 and 0.98, respectively.

The calibration results for Hombele showed R^2, NSE, and PBIAS values of 0.82, 0.82, and -2.3, respectively. These figures signify a strong fit between the simulated and observed data, with a high level of agreement between the two despite a slight underestimation of the simulated data. Melkakuntro's calibration results displayed R^2, NSE, and PBIAS values of 0.79, 0.78, and -13.1, respectively. This suggests a reasonably good fit, and explains approximately 79% of the variability in the observed data. However, the PBIAS value indicated a more significant underestimation of the simulated data than that of the observed values.

During the validation, both Hombele and Melkakuntro exhibited satisfactory results. The Hombele's R^2, NSE, and PBIAS values were 0.71, 0.67, and 11.2, respectively, indicating a reasonable fit between the simulated and

observed data. Melkakuntro showed R^2, NSE, and PBIAS values of 0.7, 0.66, and 1.9 respectively, demonstrating good agreement between the simulated and observed data.

The SWAT model findings revealed that the mean annual recharge in the upper wash sub-basin is approximately 181.1 mm/year, accounting for 2.1 BCM/year and constituting approximately 19.1% of the total mean annual precipitation. The simulated mean annual surface runoff was 93.4 mm, or roughly 1.09 BCM, representing 9.4% of the mean annual precipitation. Evapotranspiration was estimated at 682.5 mm/year, making up 71.5% of the mean annual precipitation and the annual average total water yield was 233.5 mm in the upper Awash sub-basin. The ability of the model to represent processes spatially allows for an accurate depiction of spatial heterogeneity. These quantitative findings offer actionable insights into water allocation planning, drought preparedness, and ecosystem sustainability.

The findings of this study contribute to a novel understanding of the temporal and spatial distribution of water budget components and water yield of the upper wash river subbasin. The hydrological sensitivity of the basin to land use, climate, and topographic properties was revealed using the SWAT model, which was calibrated with long-term data. It is interesting that as groundwater recharge is low, surface runoff is small, and evapotranspiration dominates the water budget, the role of integrated land and water management practices is further emphasized, and further research is required to integrate climate change projections, land use scenario modelling, and socio-hydrological interactions to develop adaptive water management. Inclusion of remote sensing-derived datasets and field-based recharge measurements and coupling with GW flow models may enhance estimates of recharge dynamics and storage sustainability. Their efforts will be a step forward in scientific analysis that will facilitate policy-making to alleviate water stress and ensure sustainable water yield under data-poor circumstances such as the Upper Awash.

Highlights

- Applied the SWAT model to assess water budget components in Ethiopia's Upper Awash Sub-Basin using 28 years of data.
- Calibrated and validated SWAT at two stations with strong performance metrics ($R^2 > 0.7$, NSE > 0.66).
- Sensitivity and uncertainty analyses identified the key parameters influencing the streamflow in a data-scarce basin.
- Evapotranspiration dominated the water budget, accounting for 71.8% of annual rainfall.
- The results support sustainable water management and planning in the climate- and land-use-sensitive Ethiopian highlands.

Conflicts of Interest

The authors declare that they have no known competing financial interests or personal relationships that could influence the work reported in this study.

Funding

This study did not receive external funding.

Acknowledgments

The authors would like to express their gratitude to the Water and Energy Design and Supervision Works Sector (ECDSWC-WEDSWS) of the Ethiopian Construction Design and Supervision Corporation, Ethiopian National Meteorological Agency (NMA), and the Ministry of Water and Energy (MoWE) for their valuable contribution to daily weather and river flow data.

Author Contributions

Muauz Amare Redda: Conceptualization; Methodology; Software; Formal Analysis; Data Curation; Writing - Original Draft, Behailu Berehanu: Conceptualization; Methodology; Supervision; Writing - Review & Editing, and Bedru Husien: Methodology; Supervision; Writing - Review & Editing.

References

[1] UN-Water. Integrated Monitoring Guide for Sustainable Development Goal 6. Water Sanit. 2018;

[2] FAO. Coping with water scarcity: An action framework for agriculture and food security. 2012.

[3] Luttinen A, Kurhila M, Puttonen R, Whitehouse M, Andersen T. Periodicity of Karoo rift zone magmatism inferred from zircon ages of silicic rocks: Implications for the origin and environmental impact of the large igneous province. J Afr Earth Sci. 2008; 52(3): 165-73. http://doi:10.1016/j.jafrearsci.2008.06.002

[4] Liang C, Zhang X, Xia J, Xu J, She D. The effect of sponge city construction for reducing directly connected impervious areas on hydrological responses at the urban catchment scale. Water. 2020; 12(4): 1163. http://doi:10.3390/w12041163

[5] Siekmann T, Siekmann M. Resilient urban drainage – Options of an optimized area-management. Urban Water J. 2021; 18(4): 247-64. http://doi:10.1080/1573062X.2021.1886430

[6] Aboelnour M, Engel BA, Frisbee M, Gitau M. Impacts of watershed physical properties and land use on baseflow at regional scales. J Hydrol Reg Stud. 2021; 35: 100810. http://doi:10.1016/j.ejrh.2021.100810

[7] Arnold JG, Moriasi DN, Gassman PW, Abbaspour KC, White MJ, Srinivasan R, *et al*. SWAT: Model use, calibration, and validation. Trans ASABE. 2012; 55(4): 1491-508. https://doi.org/10.13031/2013.42256

[8] Gassman PW, Reyes MR, Green CH, Arnold JG. The Soil and Water Assessment Tool: Historical development, applications, and future research directions. Trans ASABE. 2007; 50(4): 1211-50. http://dx.doi.org/10.13031/2013.23637

[9] Roushangar K, Alizadeh F. Using multi-temporal analysis to classify monthly precipitation based on maximal overlap discrete wavelet transform. Hydrol Res. 2019; 50(5): 1451-68. http://doi:10.2166/nh.2019.021

[10] Bewket W, Conway D. A note on the temporal and spatial variability of rainfall in the drought-prone Amhara region of Ethiopia. Int J Climatol. 2007; 27(11): 1467-77. https://doi.org/10.1002/joc.1481

[11] Dile YT, Berndtsson R, Setegn SG. Hydrological response to climate change for Gilgel Abay River, in the Lake Tana Basin – Upper Blue Nile Basin of Ethiopia. PLoS One. 2013; 8(10): e79296. http://doi:10.1371/journal.pone.0079296

[12] Sola F, Vallejos A, López-Geta JA, Pulido-Bosch A. The role of aquifer media in improving the quality of seawater feed to desalination plants. Water Resour Manage. 2013; 27(5): 1377-92. https://doi.org/10.1007/s11269-012-0243-6

[13] Sanchez R, Rodriguez L, Tortajada C. Transboundary aquifers between Chihuahua, Coahuila, Nuevo Leon and Tamaulipas, Mexico, and Texas, USA: Identification and categorization. J Hydrol Reg Stud. 2018; 20: 74-102. https://doi.org/10.1016/j.ejrh.2018.04.004

[14] Lyon SW, Laudon H, Seibert J, Mörth M, Tetzlaff D, Bishop KH. Controls on snowmelt water mean transit times in northern boreal catchments. Hydrol Process. 2010; 24(12): 1672-84. doi:10.1002/hyp.7577

[15] Zubieta R, Molina-Carpio J, Laqui W, Sulca J, Ilbay M. Comparative analysis of climate change impacts on meteorological, hydrological, and agricultural droughts in the Lake Titicaca basin. Water. 2021; 13(2): 175. https://doi.org/10.3390/w13020175

[16] Vorosmarty CJ, McIntyre PB, Gessner MO, Dudgeon D, Prusevich A, Green P, *et al*. Global threats to human water security and river. Nature. 2010; 555-61. https://doi.org/10.1038/nature09440

[17] Wada Y, van Beek LPH, Bierkens MFP. Modelling global water stress of the recent past: on the relative importance of trends in water demand and climate variability. Hydrol Earth Syst Sci. 2011; 15(12): 3785-808. https://doi.org/10.5194/hess-15-3785-2011

[18] Rani S, Sreekesh S. Evaluating the responses of streamflow under future climate change scenarios in a Western Indian Himalaya watershed. Environ Process. 2019; 6: 155-74. https://doi.org/10.1007/s40710-019-00361-2

[19] Gleeson, T, Wada, Y, Bierkens M, van Beek LPH. Water balance of global aquifers revealed by groundwater footprint. Nature. 2012; 488: 197-200. https://doi.org/10.1038/nature11295

[20] Alifujiang Y, Lu N, Feng P, Jiang Y. China's urban water utilization based on the water footprint methodology. Water. 2024; 16(3): 462. https://doi.org/10.3390/w16030462

[21] Kebede S, Travi Y, Alemayehu T, Ayenew T. Groundwater recharge, circulation and geochemical evolution in the source region of the Blue Nile River, Ethiopia. Appl Geochem. 2005; 20(9): 1658-76. https://doi.org/10.1016/j.apgeochem.2005.04.016

[22] Hanasaki T, Fujimori S, Yamamoto T, Yoshikawa S, Masaki Y, Hijioka Y *et al*. A global water scarcity assessment under shared socioeconomic pathways–Part 1. Hydrol Earth Syst Sci. 2013; 17: 2375-91. https://doi.org/10.5194/hess-17-2375-2013

[23] Allen RG, Pereira LS, Raes D, Smith M. Crop evapotranspiration-Guidelines for computing crop water requirements-FAO Irrigation and drainage paper 56. Room: FAO - Food and Agriculture Organization of the United Nations; 1998 Jan 1, M-56. Available from: http://www.fao.org/3/x0490e/x0490e00.htm

[24] Gulakhmadov T, Kienzler KM, Eschanov R, Akramkhanov A, Toderich KN, Martius C Assessing the potential impacts of climate change on water resources using SWAT model: a case study from the Amudarya River Basin, Central Asia. Environ Earth Sci. 2020; 79: 177. http://doi: 10.1007/s12665-020-08914-7

[25] Monteith JL. Evaporation and environment. In: Fogg GE, Ed. The State and Movement of Water in Living Organisms. Symposium of the Society for Experimental Biology, vol. 19; London: Academic Press Inc.; 1965, pp. 205-34.

[26] Arnold JG, Allen. PM. Automated methods for estimating baseflow and groundwater recharge from stream flow records. J Amer Water Resour Assoc. 1999; 35(2): 411-24. https://doi.org/10.1111/j.1752-1688.1999.tb03599.x

[27] Winchell M, Srinivasan R, Di Luzio M, Arnold JG. ArcSWAT interface for SWAT2005: User's guide. Temple, TX: Blackland Research Center, Texas Agricultural Experiment Station, USDA-ARS; 2007.

[28] Neitsch SL, Arnold JG, Kiniry JR, Williams JR. Soil and Water Assessment Tool: Theoretical Documentation, Version 2005. Temple, TX: Grassland, Soil and Water Research Laboratory; Agricultural Research Service; January 2005. Available from: https://swat.tamu.edu/media/1292/swat2005theory.pdf

[29] Nachtergaele F, van Velthuizen H, Verelst L BN. Harmonized World Soil Database (version 1.2). FAO, Rome, Italy IIASA, Laxenburg, Austria [Internet]. 2012;1–50. Available from: http://www.fao.org/nr/water/docs/harm-world-soil-dbv7cv.Pdf

[30] Chow VT, Maidment DR, Mays LW. Applied Hydrology. New York: McGraw-Hill; 1988. P. 572.

[31] van Griensven A, Meixner T, Grunwald S, Bishop T, Diluzio M, Srinivasan R. A global sensitivity analysis tool for the parameters of multi-variable catchment models. J Hydrol. 2006; 324(1-4): 10-23. https://doi.org/10.1016/j.jhydrol.2005.09.008

[32] Karim C. Abbaspour, Yang J, Maximov I, Siber R, Bogner K, Mieleitner J. Modelling hydrology and water quality in the pre-alpine/alpine Thur watershed using SWAT. J Hydrol. 2007; 333(2-4): 413-30. https://doi.org/10.1016/j.jhydrol.2006.09.014

[33] Abbaspour KC, Rouholahnejad E, Vaghefi S, Srinivasan R, Yang H, Klove B. A continental-scale hydrology and water quality model for Europe: Calibration and uncertainty of a high-resolution large-scale SWAT model. J Hydrol. 2015; 524: 733-52. https://doi.org/10.1016/j.jhydrol.2015.03.027

[34] Moriasi DN, Arnold JG, Van Liew MW, Bingner RL, Harmel RD, Veith TL. Model evaluation guidelines for systematic quantification of accuracy in watershed simulations. Trans ASABE. 2007; 50(3): 885-900. https://doi.org/10.13031/2013.23153

[35] Santhi C, Arnold JG, Williams JR, Dugas WA, Srinivasan R, Hauck LM. Validation of the SWAT model on a large river basin with point and nonpoint sources. JAWRA J Am Water Resour Assoc. 2001; 37: 1169-88. https://doi.org/10.1111/j.1752-1688.2001.tb03630.x

[36] Nash JE, Sutcliffe JV. River flow forecasting through conceptual models part I — A discussion of principles. J Hydrol. 1970; 10(3): 282-90. https://doi.org/10.1016/0022-1694(70)90255-6

[37] Gupta HV, Sorooshian S, Yapo PO. Status of automatic calibration for hydrologic models: comparison with multilevel expert calibration. J Hydrol Eng. 1999; 4(2): 135-43. https://doi.org/10.1061/(ASCE)1084-0699(1999)4:2(135)

[38] Neitsch SL, Arnold JG, Kiniry JR, Williams JR. Soil & Water Assessment Tool Theoretical Documentation Version 2009. Soil & Water Assessment Tool Theoretical Documentation Version 2009; 2011; TR No. 406. Available from: https://swat.tamu.edu/media/99192/swat2009-theory.pdf

[39] Mockus V, McKeever V, Owen W, Rallison R. Section 4: Hydrology. In: National Engineering Handbook, Part 630: Hydrology. Washington DC: U.S. Soil Conservation Service; 1969.

[40] Arnold JG, Muttiah RS, Srinivasan R, Allen PM. Regional estimation of base flow and groundwater recharge in the Upper Mississippi river basin. J Hydrol. 2000; 227: 21-40. https://doi.org/10.1016/S0022-1694(99)00139-0

[41] Venetis C. A study of the recession of unconfined aquifers. Assoc Sci Hydrol. 1969; 14(4): 119-25. https://doi.org/10.1080/02626666909493759

[42] Wang Y, Gu X, Yang G, Yao J, Liao N. Impacts of climate change and human activities on water resources in the Ebinur Lake Basin, Northwest China. J Arid Land. 2021; 13: 581-98. https://doi.org/10.1007/s40333-021-0067-4